Full title:

Sex differences in change-of-mind neuroeconomic decision-making is modulated by LINC00473 in medial prefrontal cortex

Short title:

Neuroeconomic decision-making in males and females

Authors:

Romain Durand-de Cuttoli[1], Orna Issler[2], Benjamin Yakubov[3], Nusrat Jahan[3], Aisha Abid[3], Susanna Kasparov[3], Kastalia Granizo[3], Sanjana Ahmed[3], Scott J. Russo[1], Eric J. Nestler[1,4], Brian M. Sweis*[1,4]

*Corresponding: brian.sweis@mountsinai.org

Affiliations:

[1] Nash Family Department of Neuroscience, Friedman Brain Institute, Icahn School of Medicine at Mount Sinai, New York, NY 10029

[2] Neuroscience Institute, Department of Anesthesiology, Perioperative Care and Pain Medicine, and Department of Neuroscience and Physiology, NYU Langone, New York, NY 10016

[3] CUNY Hunter, New York, NY 10023

[4] Department of Psychiatry, Icahn School of Medicine at Mount Sinai, New York, NY 10029

Abstract:

Changing one's mind is a complex cognitive phenomenon involving a continuous re-appraisal of the trade-off between past costs and future value. Recent work modeling this behavior across species has established associations between aspects of this choice process and their contributions to altered decision-making in psychopathology. Here, we investigated the actions in medial prefrontal cortex (mPFC) neurons of long intergenic non-coding RNA, LINC00473, known to induce stress resilience in a striking sex-dependent manner, but whose role in cognitive function is unknown. We characterized complex decision-making behavior in male and female mice longitudinally in our neuroeconomic foraging paradigm, Restaurant Row, following virus-mediated LINC00473 expression in mPFC neurons. On this task, mice foraged for their primary source of food among varying costs (delays) and subjective value (flavors) while on a limited time-budget during which decisions to accept and wait for rewards were separated into discrete stages of primary commitments and secondary re-evaluations. We discovered important differences in decision-making behavior between female and male mice. LINC00473 expression selectively influenced multiple features of re-evaluative choices, without affecting primary decisions, in female mice only. These behavioral effects included changing how mice (i) cached the value of the passage of time and (ii) weighed their history of economically disadvantageous choices. Both processes were uniquely linked to change-of-mind decisions and underlie the computational bases of distinct aspects of counterfactual thinking. These findings reveal a key bridge between a molecular driver of stress resilience and psychological mechanisms underlying sex-specific decision-making proclivities.

41 **Introduction:**

42

43 How an individual changes one's mind when making choices is a challenging yet important
44 phenomenon that has been gaining more traction recently in the field of decision science [1]. This mental
45 process involves complex interactions between cognitive and affective systems and presents an
46 opportunity to peer into how the brain represents internal conflict [2, 3]. This captures conflict at multiple
47 levels, including the economic level: between competing interests of managing ongoing expenditures while
48 minimizing potential losses vs. maximizing future gains [4], as well as the psychological level: re-evaluating
49 one's own recent actions, which could be perceived as egodystonic [5-7]. Aspects of these processes are
50 likely dysfunctional in psychiatric illnesses and may manifest as the cognitive changes observed in mood
51 disorders like depression, considering these mental operations could contribute to affective burden [8, 9].
52 While the neural mechanisms underlying change-of-mind decision-making remain underexplored,
53 expanding this line of investigation holds promise to enrich our understanding of the repertoire of behavioral
54 processes at play in depression.

55

56 Depression is a debilitating mental illness characterized by pervasive mood disturbances, altered
57 cognitive capabilities, and maladaptations in motivated behavior [9]. The incidence of depression is two
58 times higher in women than in men and can manifest different symptomatology, including negative
59 rumination [10]; however, the molecular mechanisms mediating these sex differences are unclear [11-15].
60 Progress is being made toward appreciating neuroanatomical, genetic, epigenetic, and pathophysiological
61 differences between depressed males and females based on advances in clinical and preclinical research,
62 with the latter enabling mechanistic studies of sex as a biological factor [16, 17]. Such advances are also
63 due to adopting novel approaches that leverage unsupervised analyses of large datasets in emerging fields
64 of systems biology leading to breakthroughs, for example, in identifying key regulatory roles of non-coding
65 elements of the genome [18].

66

67 Recent transcriptomics work carried out in human postmortem brain tissue samples obtained from
68 subjects carrying a diagnosis of major depressive disorder discovered sex-dependent functions of a

69 primate-specific long intergenic non-coding RNA: LINC00473 [19]. Overall, long non-coding RNAs
70 represent a significant percentage of all of the regulated transcripts in human depression and are regulated
71 in a sex- and brain region-specific manner. [19]. Lower LINC00473 expression levels were found in the
72 medial prefrontal cortex (mPFC) of depressed females only [19]. Cross-species validation studies in rodents
73 demonstrated expressing LINC00473 in mPFC neurons promotes resilience to stress in females only [19].
74 This included ameliorating depressive- and anxiety-like behaviors while blunting hypothalamic-pituitary-
75 adrenal-axis activity as well as the induction of gene expression changes induced by chronic stress [19].
76 Other studies have implicated LINC00473 in molecular scaffolding, inter-organelle communication, and
77 transcriptional regulation in non-neuronal tissue, while exhibiting immediate early gene-like properties in
78 cultured neurons [20-25]. Beyond this, LINC00473 has not been studied in neural tissue in any other
79 capacity, with no work performed to date on the role of long non-coding RNAs in regulating decision-making
80 information processing.
81
82 Strides made in the field of neuroeconomics, an area focused on understanding how the brain is
83 comprised of multiple valuation algorithms, have leveraged complex approaches in decision neuroscience
84 to quantify how circuits constrain behavior [26-29]. This encompasses characterizing multifactorial aspects
85 of motivation that operationalize reward value along several dimensions, integrate choice processes with
86 environmental circumstances, and segregate stages of a decision stream into its component parts [30-33].
87 This work includes isolating properties of change-of-mind re-evaluative decisions, and points to the mPFC
88 as a critical hub for regulating reward value, self-control, and mood [4, 34-38]. Insights from neuroeconomic
89 principles offer novel approaches to investigate decision-making capable of resolving behavior into
90 discretely measurable computational units in a manner that is biologically tractable and readily translatable
91 across species [30, 39, 40]. This approach has yielded efforts from our team and others developing
92 innovative tasks adapted for use in mice, rats, monkeys, and humans [5, 41-44]. The use of these
93 translational tasks have led to cross-species discoveries uncovering the behavioral underpinnings of
94 signatures of higher-order cognitive processes, previously thought to be unique to humans, supported by
95 physically separable circuits in the brain [45-49].
96

97 Here, we characterized complex decision-making behavior in mice tested on our longitudinal
98 neuroeconomic foraging paradigm, Restaurant Row. This task has been utilized previously to gain access
99 to behavioral and neurophysiological correlates of multiple decision-making systems in the brain, including
100 fundamentally distinct valuation algorithms engaged within the same trial [5, 47, 50-55]. On this task,
101 rodents forage for their primary source of food among varying costs (delays cued by tone pitch) and
102 subjective value (flavors tied to spatially fixed and contextualized locations, or "restaurants") while on a
103 limited time-budget. Decisions to accept and wait for rewards are separated into discrete stages of primary
104 commitment (accept vs. reject in an offer zone) and secondary re-evaluation (stay vs. quit in a wait zone).
105 We tested both male and female mice – the first ever analysis of females in this task – transfected with a
106 newly packaged adeno-associated virus expressing LINC00473 or only a green fluorescent protein targeted
107 to mPFC neurons (**Fig. 1a**, **Supplementary Fig. 1**). Mice were tested daily over two months across a
108 changing economic landscape during which complex foraging strategies developed. We report sex- and
109 LINC00473-dependent differences in neuroeconomic decision-making behavior specific to alterations in
110 multiple features of change-of-mind re-evaluative choices without affecting primary decisions. Differences
111 were rooted in dissociable forms of counterfactual thinking, or how sensitive individuals were to missed
112 opportunities for alternative actions that could have led to hypothetically better outcomes – the
113 computational basis of regret processing previously captured by leveraging this task across species [5, 45,
114 46, 48, 56, 57].

115 **Results:**

116

117 *Male and female mice similarly acquire the Restaurant Row task.*

118 All mice underwent virus transfection surgeries and were allowed 2-3 weeks to recover before
119 beginning the longitudinal Restaurant Row paradigm (**Fig. 1a**). During the first week of Restaurant Row
120 testing, all reward offers were fixed at 1 s only (cued by a 4 KHz tone) as mice acquired the basic structure
121 of the task (**Fig. 1a-b**), learning to run in the correct direction to forage for low-cost food rewards. All mice
122 were food restricted to the same percentage (~80-85%) of baseline free-feeding weight (**Supplementary**
123 **Fig. 2**). Both males and females, regardless of GFP or LINC00473 treatment, grossly traveled similar total
124 distances across the first week (**Fig. 1c**, sex*virus: F=0.971, p=0.331). Behavior shaped equally among all
125 groups as the number of laps run in the correct direction (**Fig. 1d**, day: F=334.219, p<0.0001; sex*virus:
126 F=2.780, p=0.104) and total pellets earned (**Fig. 1e**, day: F=393.991, p<0.0001; sex*virus: F=3.062,
127 p=0.089) increased across the first week. All mice displayed subjective flavor preferences, revealed by
128 splitting earnings among flavors ranked from least to most preferred by summing end-of-session totals in
129 each restaurant (**Fig. 1f**, rank: F=255.250, p<0.0001). There was a modest upward shift in earns split by
130 flavor ranking in LINC00473-treated females across the first week (**Fig. 1f**, sex*virus: F=3.334, p=0.076).
131 Overall, these data indicate all groups were able to demonstrate the ability to acquire the basic structure of
132 the task and forage for food in a self-paced manner without overt locomotor or gross feeding differences.

133

134 *LINC00473 alters value-dependent, task-driven conditioned place preference behavior in females.*

135 Before and after the first week of behavioral testing, we characterized exploratory behavior in the
136 maze arena (**Fig. 2a-b**). That is, without any active task, mice were allowed to roam the maze freely on day
137 0 and again on day 8 of the experimental timeline (**Fig. 2b**). This allowed us to probe a conditioned place
138 preference (CPP) response for reward sites driven by experience that naturally developed throughout the
139 first week of self-paced task performance. We measured the number of entries into and time spent near
140 the feeder site in each restaurant's wait zone on these two probe sessions (**Fig. 2c-e**). All mice explored
141 the arena, including each restaurant, to similar degrees at baseline (day 0) and did not differ between
142 groups (sex*virus [entries]: F=0.259, p=0.614; sex*virus [time]: F=1.155, p=0.290, **Fig. 2c**). Overall,

143 compared to the day 0 pre-test baseline, we found that during the day 8 post-test all mice robustly increased
144 total time spent (F=75.818, p<0.0001) and to a lesser degree entries into the reward sites F=8.501, p<0.01,
145 **Fig. 2c**). We then split these metrics by restaurant ranked according to day 7's task earnings and found
146 that CPP scores scaled with flavor preferences (rank [entries]: F=16.307, p<0.0001; rank [time]: F=9.829,
147 p<0.0001, **Fig. 2f-g**). We found significantly lower CPP scores (post-pre delta score of 0 on average) with
148 respect to time spent in the wait zone of the most preferred flavor in LINC00473-treated females only,
149 despite being matched to males for equivalent number of rewards earned on day 7 of the task
150 (sex*virus*rank [time]: F=2.844, p<0.05, **Fig. 2f-g**). This sex-dependent effect was replicated in an
151 independent cohort of mice separately transfected with a lower titer of the AAV-expressing LINC00473
152 (**Supplementary Fig. 3**). Conversely, LINC00473-treated females displayed a higher number of post-pre
153 test entries into less preferred restaurants compared to males or GFP controls (sex*virus*rank [entries]:
154 F=5.584, p<0.001, **Fig. 2f-g**, **Supplementary Fig. 3**). These findings highlight that mPFC LINC00473
155 expression can have sex-specific effects on select actions during value-based reward-seeking behavior.
156 More specifically, LINC00473 treatment in females altered preference-dependent entering vs. exiting
157 choices that may access dissociable computations involved in checking-waiting-leaving behavioral
158 sequences [51, 58, 59], shedding light on more discrete interpretations of CPP metrics than are traditionally
159 reported in simpler assays and explored in detail below.
160
161 *Escalating reward scarcity unmasks sex-dependent effects of LINC00473 on complex foraging profiles.*
162 We next examined task foraging profiles across the subsequent weeks as we increased the
163 distribution of offer costs (the presented delays) available in the task environment without adjusting the
164 limited time budget mice had to forage for food (**Fig. 3a**). Thus, in this closed-economy system, tightening
165 budget constraints pressured animals to adapt to the changing landscape of the environment as reward
166 scarcity increased – a model of economic stress we recently characterized [33]. Costs increased in a
167 stepwise manner across blocks of days (i.e., offer delays ranged from 1-5 s on days 8-12, 1-15 s on days
168 13-17, and finally 1-30 s on days 18-45, as previously published [5, 33, 60]) and were randomly sampled
169 from a uniform distribution (the starting offer of each longer delay is associated with a discretely higher tone
170 pitch that is presented in the offer zone and counts down in the wait zone). As expected, we found a

171 decrease in pellets earned in response to each stepwise economic challenge (sign test [-] on earns: day
172 after minus day before transition, collapsed across epochs: t=-12.655, p<0.0001, **Fig. 3b**). These deficits
173 in earnings scaled by flavor and were matched between all groups (rank: F=6.938, p<0.001, timepoint*rank:
174 F=3.651, p<0.01; sex*virus: F=0.016, p=0.899, **Fig. 3c-d**, **Supplementary Fig. 4**). The most striking
175 change in foraging behavior that accounted for environmental scarcity-induced reward deficits across the
176 experiment was the proportion of session time re-allocated to quitting behavior in the wait zone, which
177 significantly increased at each economic challenge step and more prominently in females
178 (timepoint*choice: F=226.523, p<0.0001; timepoint*sex [quits]: F=11.821, p<0.0001, **Fig. 3e**,
179 **Supplementary Fig. 4**). Across the final epoch of testing (the 1-30 s offer range period: days 18-45), mice
180 displayed a complex behavioral response profile, including running more laps that developed over multiple
181 weeks in an effort to recover and increase total food earnings (laps [days 18-45]: F=355.340, p<0.0001;
182 earns [days 18-14]: F=252.218, p<0.0001, **Fig. 3b-d**). All groups were matched in their ability to recover
183 earnings (sex*virus: F=0.234, p=0.631, **Fig. 3d**, **Supplementary Fig. 4**). However, we found that females
184 displayed a greater increase in the number of laps run compared to males throughout this process (sex*day:
185 F=7.848, p<0.01, **Fig. 3b**,**f**, **Supplementary Fig. 4**). Interestingly, LINC00473-expressing females
186 displayed a significantly higher propensity to engage in wait zone quitting behavior compared to males
187 (sex*virus: F=8.201, p<0.01, **Fig. 3g**, **Supplementary Fig. 5**). Furthermore, LINC00473-expressing
188 females displayed shorter latencies to quit upon arrival once in the wait zone compared to males particularly
189 for more preferred flavors (sex*virus*day*rank: F=2.805, p<0.05), despite no changes in offer zone reaction
190 times (F=1.713, p=0.162, **Supplementary Fig. 5**). Taken together, these data reflect rearrangements in
191 complex foraging patterns that emerged across longitudinal time scales in response to worsening economic
192 demand. These analyses reveal sex-dependent effects of mPFC LINC00473 expression that alter quit
193 decisions and are not unmasked until mice encounter a reward-scarce environment. This effect of
194 LINC00473 in the wait zone is reminiscent of the altered check-then-leave behaviors in LINC00473-
195 expressing females during the CPP probe session (see **Fig. 2**)
196
197 *Females demonstrate unique neuroeconomic decision-making policies during change-of-mind choices.*

198 To characterize the economic nature of the decisions made during distinct action-selection
199 processes in the offer zone and wait zone, we quantified choice outcomes to enter vs. skip (offer zone) or
200 earn vs. quit (wait zone) separated by both the cued offer cost and flavor identity (**Fig. 4a-c**). All mice
201 acquired the economic structure of the task, making cost-informed enter vs. skip choices in the offer zone
202 or earn vs. quit choices in the wait zone, discriminating tones as well as demonstrating different degrees of
203 willingness to wait in each restaurant (offer*flavor [offer zone]: F=13.129, p<0.001; offer*flavor [wait zone]:
204 F=18.006, p<0.001, **Fig. 4a-c**). Thresholds of willingness to accept and separately wait for offers can be
205 calculated independently in the offer zone and wait zone by fitting a Heaviside step regression to the choice
206 outcome as a function of cost and extracting the inflection (indifference) point in each restaurant (**Fig. 4d**).
207 Overall, in all mice, we found that offer zone and wait zone thresholds significantly differed from each other
208 in magnitude of response to the changing economic landscape (timepoint*zone: F=296.648, p<0.0001, **Fig.**
209 **4d**). Upon transitioning to the 1-30 s epoch of testing (day 18), offer zone thresholds drastically increased
210 in all groups to similar degrees while retaining the ordinal ranking of flavor preferences (rank: F=17.247,
211 p<0.0001; sex: F=0.170, p=0.681; sex*virus: F=0.031, p=0.861, **Fig. 4d-f**). Wait zone thresholds, on the
212 other hand, increased only in male mice following the transition to the 1-30 s epoch (rank: F=58.574,
213 p<0.0001; sex: F=17.776, p<0.0001; sex*virus: F=1.238, p=0.268, **Fig. 4d-f**). Over the subsequent week
214 (approximately days 18-24), wait zone thresholds in males decreased before stabilizing across the
215 remainder of the experiment (approximately days 25-45, **Fig. 4d-f**). In females, wait zone thresholds
216 remained relatively unchanged upon transition to day 18 and were significantly lower than males across
217 the entire 1-30 s epoch (sex*rank [offer zone]: F=0.484, p=0.694; sex*rank [wait zone]: F=3.689, p<0.05,
218 **Fig. 4d-f**). Offer zone thresholds on the other hand gradually decreased, equally in all groups, but across
219 a much slower timescale over several weeks (**Fig. 4d-f**). Leveraging an economic analysis we recently
220 developed (taking individual differences in flavor-specific earnings on day 7 and projecting profiles to the
221 decision threshold learning that takes place during the 1-30 s epoch [33]), we found that female decision-
222 making policies were more optimized for both recovering total food intake as well as yielding maximal
223 subjective value once in a reward-scarce environment (**Fig. 4g-i**, **Supplementary Fig. 6**). LINC00473
224 expression in mPFC did not significantly alter any decision-making thresholds (sex*virus [offer zone]:
225 F=1.781, p=0.185; sex*virus [wait zone]: F=187, p=0.175, **Fig. 4d-f**). These data highlight a robust sex

226 difference between distinct offer zone and wait zone decision-making processes that we previously
227 demonstrated derive from separable circuits [48, 50].
228
229 *LINC00473 in mPFC enhances change-of-mind contrast via sensitivity to sunk costs and action-specific*
230 *regret.*
231 Wait zone thresholds capture economic indifference points of re-evaluation decisions defined by
232 choice outcome as a function of the starting offer. Next, we quantified more dynamically at what timepoint
233 quit decisions were made. Thus, we calculated the value remaining in the countdown at the moment of
234 quitting by subtracting the within-trial countdown time remaining from an individual mouse's wait zone
235 threshold (**Fig. 5a**). We found all mice generally made quit decisions (i) for offers that were typically above
236 one's wait zone threshold (i.e., negatively valued offers) and (ii) with ample time remaining in the countdown
237 such that the remaining time investment required to obtain the reward was still above one's threshold (i.e.,
238 negative value left), and therefore would be economically advantageous or efficient and timesaving to quit
239 (**Fig. 5a**). Thus, overall, quit decisions reflected corrective re-evaluations of sub-optimal offer zone
240 decisions relative to one's own policy, consistent with previous reports [5, 33, 48, 49, 51]. We found that
241 females made quit decisions with significantly lower and more negative value remaining in the countdown
242 compared to males (sex*virus: F=195.823, p<0.0001, **Fig. 5b**). This sex difference was more pronounced
243 in LINC00473-expressing animals and thus made females quit decisions even more efficient compared to
244 males (sex*virus: F=12.957, p<0.001, **Fig. 5b**). Furthermore, only LINC0047-expressing mice revealed a
245 sex difference in the number of quit decisions that could be characterized as economically advantageous
246 (as described above, sex*virus: F=153.236, p<0.0001), with a greater proportion of these events in females
247 compared to other quit events that were less common and more disadvantageous (i.e., quitting negatively
248 valued offers [above one's threshold] with positive value left [below one's threshold]; or, quitting positively
249 valued offers [below one's threshold] – both reflecting quits passing the timepoint after which mice should
250 have chosen to stay instead (quit type*sex*virus: F=13.293, p<0.0001, **Fig. 5c-d**).
251
252 We then characterized the temporal dynamics of how mice made continuous re-evaluation
253 decisions in the wait zone as a function of the passage of time, which wait zone thresholds do not capture.

254 We calculated the instantaneous probability of staying and earning a reward as a continuous function of
255 not only (i) the time remaining in the countdown at each snapshot in time but also (ii) the time already spent
256 waiting. We computed a survival analysis using a sliding 1 s window after binning all trials of varying starting
257 offers into [time spent, time left] pairs (**Fig. 5f**). In all groups, we found that the passage of time drove an
258 increased likelihood that mice would continue to wait, the effect of which grew additively stronger with
259 escalating time spent independent of and orthogonal to temporal distance to the goal measured at any
260 given moment in time (time spent*time left: F=891.924, p<0.0001, **Fig. 5f-h**). This captures a well-studied
261 cognitive phenomenon known as the sunk cost bias whereby irrecoverable past expenditures can enhance
262 the value of continuing to invest in and perseverate on an ongoing endeavor, as we have reported
263 previously captured across species [46, 49]. We found a significant sex difference in sensitivity to sunk
264 costs only in LINC00473-expressing mice. LINC00473-expressing females demonstrated increased
265 sensitivity to sunk costs compared to LINC00473-expressing males, which instead demonstrated relatively
266 diminished sensitivity to sunk costs during quit decisions (sex*virus: F=15.944, p<0.0001, **Fig. 5i**). This
267 effect only emerged after mice transitioned to the 1-30 s reward-scarce environment (time spent in wait
268 zone [1-15 s offers]: F=0.174, p=0.677, **Fig. 5i**, **Supplementary Fig. 7**) and uniquely affected wait zone
269 decisions compared to other forms of time spent on this task, including in the offer zone (time spent in offer
270 zone: F=0.558, p=0.455; time spent*sex*virus: F-0.418, p-0.518, **Supplementary Fig. 7**). These data
271 highlight sex- and LINC00473-dependent alterations in how the passage of time can differentially enhance
272 reward value and escalate the commitment to an ongoing endeavor specifically during re-evaluation
273 decisions.
274
275 Next, we aimed to characterize how events related to quit decisions on a given trial influenced
276 subsequent behavior. Because trials are interdependent, a strength of the Restaurant Row task lies in being
277 able to subdivide trial sequences into unique economic scenarios in which animals naturalistically find
278 themselves. Analysis of mice after they make suboptimal choices and potentially realize when gaining
279 access to information that an alternative, unselected action could have led to a better outcome has led to
280 breakthrough discoveries modeling across species aspects of the behavioral and neurophysiological
281 signatures of counterfactual thinking – the computational basis of regret processing [5, 47, 48, 61-63]. We

282 previously linked such processes to quit decisions as well as other types of economic choices on this task
283 [5, 47, 48]. In past reports, we and others behaviorally operationalized counterfactual sensitivity on
284 Restaurant Row by identifying trial pair sequences [trial t-1 → trial t] in which animals made economically
285 suboptimal choices [on trial t-1] and by measuring the change in economic choice behavior on the next trial
286 [on trial t: the read-out trial] [5, 47, 48]. Importantly, these events are compared to specific control sequences
287 that remove the error of one's own agency by examining non-violation events [on trial t-1], matched for all
288 other economic factors (e.g., including the offer values and flavor identities on both trials t-1 and trial t) in
289 order to behaviorally measure changes in decision-making counterfactual based on one's choice history:
290 our operational behavioral definition of counterfactual sensitivity. Recent work demonstrated the importance
291 of the mPFC in these behavioral sensitivity measures on our neuroeconomic task [48]. Sequences were
292 extracted post hoc from natural encounters while foraging amid randomly presented offers, not constructed
293 a priori nor built into the task design.
294
295 We previously defined two distinct regret-related sequences of events on this task [5, 47, 48].
296 **Scenario 1**: situations in which animals inappropriately forgo a high-value offer [on trial t-1] only to
297 subsequently encounter a worse low-value offer on the next trial [trial t] (**Fig. 5j**). This violation sequence
298 can be compared to the non-violation control sequence in which mice instead appropriately accepted the
299 high-value offer on trial t-1, holding all other variables constant (**Fig. 5j**). Here, we found that all groups
300 were insensitive to scenario 1, with no effect of sex or LINC00473 expression (+ sign test: [male GFP]: t=-
301 0.282, p=0.608; [female GFP]: t=0.101, p=0.461; [male LINC]: t=0.521, p=0.308; [female LINC]: t=-0.144,
302 p=0.556, **Fig. 5j**). That is, there were no changes in economic choice behavior on the read-out trial when
303 comparing violation sequences to non-violation sequences [thus yielding a delta score of zero in change of
304 choice probabilities on trial t] (**Fig. 5j**). **Scenario 2**: situations in which animals inappropriately accepted a
305 low-value offer [on trial t-1] that typically precipitates a resultant change-of-mind decision (**Fig. 5k**). This
306 violation sequence can be compared to the non-violation control sequence in which mice instead
307 appropriately skipped the low-value offer on trial t-1, holding all other variables constant and matched for
308 the same low-value offer on trial t as in scenario 1 (**Fig. 5j-k**). Overall, we found that mice demonstrated
309 sensitivity to scenario 2, whereby individuals were more likely to compensate for and accept low-value

310 offers that they typically would not on the read-out trial following violation sequences compared to non-
311 violation sequences (**Fig. 5k**). Interestingly, only GFP-treated females did not display scenario 2 sensitivity,
312 while all other groups including LINC00473-expressing females displayed delta scores significantly greater
313 than zero (+ sign test: [male GFP]: t=2.931, p<0.01; [female GFP]: t=1.123, p=0.145; [male LINC]: t=3.056,
314 p<0.01; [female LINC]: t=2.196, p<0.05, **Fig. 5k**). Taken together, these data reveal how mice can
315 differentially carry the weight of distinct types of past mistakes into future choices, with a unique association
316 between change-of-mind-related counterfactual sensitivity (scenario 2, not scenario 1) and mPFC
317 LINC00473 expression in females. These findings provide an example whereby LINC00473 expression in
318 this brain region overcomes a baseline sex difference that potentially normally disadvantages females.
319
320 Lastly, we characterized how access to task-relevant information may be critically important for
321 sex- and LINC00473-dependent differences during change-of-mind decisions. After day 45, we tested mice
322 for an additional 2 days during which tone playback on the task was silenced only in the wait zone but
323 remained audible during offer zone presentations (**Fig. 6a**). That is, mice had access to cost information
324 signaled by tone pitch when making initial enter vs. skip decisions in the offer zone, but received no
325 countdown information once in the wait zone while making secondary re-evaluative decisions to quit or stay
326 before earning rewards. Overall, we found that males were more sensitive to this informational manipulation
327 compared to females. Both GFP- and LINC00473-expressing males displayed a modest decreased number
328 of laps run and total number of pellets earned, while female mice remained relatively unchanged between
329 audible and silent conditions (laps [timepoint*sex]: F=10.678, p<0.01; laps [timepoint*virus]: F=0.449,
330 p=0.507; earns [timepoint*sex]: F=10.124, p<0.01; earns [timepoint*virus]: F=0.002, p=0.969, **Fig. 6b-c**).
331 This task manipulation did not alter any overt changes in offer zone choices in any group as animals
332 continued to discriminate the audible tones during cost-informed enter vs. skip decisions (offer:
333 F=1186.818, p<0.0001; offer*timepoint: F=1.365, p=0.243; **Fig. 6d**). Interestingly, when examining changes
334 in wait zone thresholds, we found a significant sex difference when wait zone countdown information was
335 withheld that was compounded by an additional LINC00473 effect in females only (**Fig. 6e**). In males,
336 compared to the audible condition, the lack of auditory information cuing mice on progress during the
337 countdown in the silent wait zone condition drove an increase in wait zone thresholds for most preferred

338 flavors (timepoint: F=22.976, p<0.0001; timepoint*virus: F=0.181, p=0.671 **Fig. 6e**). Males also displayed
339 a concomitant decrease in wait zone thresholds for least preferred flavors (timepoint: F=19.561, p<0.0001;
340 timepoint*virus: F=0.526, p=0.470, **Fig. 6e**). These data indicate that, without cued auditory guidance in the
341 wait zone, males were more patient waiting for favorite flavors and less patient waiting for least favorite
342 flavors (defined by a change in the indifference point of earn outcomes as a function of the trial's starting
343 offer). Conversely, GFP-expressing females only displayed a decrease in wait zone thresholds for less
344 preferred flavors, with no change in thresholds for most preferred flavors (**Fig. 6e**). LINC00473-expressing
345 females however did not display any changes in wait zone thresholds in any restaurant compared between
346 audible and silent wait zone conditions (timepoint [most preferred]: F=2.569, p=0.112; timepoint*virus [most
347 preferred]: F=0.137, p=0.712; timepoint [least preferred]: F=12.185, p<0.0001; timepoint*virus [least
348 preferred]: F=8.901, p<0.01). These data indicate LINC00473-expressing females valued offers in a
349 consistent manner with or without externally guided information, suggesting that their internal measures of
350 time or how they hold and maintain information from the offer zone in working memory may be more stable.
351 When examining quit times in the wait zone, all mice displayed a modest increased latency to make quit
352 decisions in the silent condition compared to the audible condition (timepoint: F=11.764, p<0.001; sex:
353 F=2.358, p=0.126; virus: F=0.836, p=0.361, **Fig. 6f**). Finally, when examining sensitivity to sunk costs, we
354 found that the silent condition unmasked a sex difference in GFP-treated mice whereby females show
355 increased sunk cost sensitivity as a function of the passage of time compared to males – a sex difference
356 that was previously only apparent during the audible condition in LINC00473-expressing groups (time
357 spent: F=97.196, p<0.001; sex: F=36.989, p<0.0001; virus: F=1.899, p=0.168; **Fig. 6g**, see
358 **Supplementary Fig. 8** for alternate task information manipulations). Taken together, these findings
359 highlight the complexity of change-of-mind decisions, how mice internally generate value representations
360 with vs. without access to explicit, exogenous task-relevant information, and the multifactorial ways in which
361 this re-evaluative choice process can be uniquely modulated in a sex-dependent manner.

362 **Discussion:**

363

364 In this study, we characterized highly complex behaviors in mice tested on the neuroeconomic
365 foraging paradigm, Restaurant Row. We explored the role of a non-coding RNA, a relatively poorly
366 understood class of molecules, on motivated behavior. We discovered sex-dependent effects of LINC00473
367 expression in mPFC neurons on specific aspects of value-based decision-making information processing.
368 This was typified by selectively altering the way in which an individual changes one's mind during an
369 ongoing decision. Importantly, we discovered a role for mPFC LINC00473 expression – which we recently
370 found increases stress resilience in simple behavioral screening tests in female mice only [19] – in
371 sharpening the contrast of re-evaluation processes in females. Our findings extend from simple conditioned
372 place preference behaviors like those commonly assayed using simpler goal-oriented paradigms [40, 64,
373 65] to more complex, higher order neuroeconomic phenomena. These latter effects included enhancing
374 specific aspects of sensitivity to sunk costs and counterfactual thinking. These data provide a deeper
375 understanding of how multiple stages of a continuous decision stream derive from dissociable psychological
376 mechanisms supported by physically separable circuits in the brain. Our findings have important
377 implications for how molecular determinants of stress responses and non-coding regions of the genome
378 can influence changes in motivated behavior via unique region-specific decision-making computations
379 differentially leveraged by males and females.

380

381 The distinction between offer zone choices and wait zone choices on the Restaurant Row task is
382 critically important. They reflect a separation of fundamentally distinct decision-making algorithms that occur
383 within the same trial but are segregated across space and time [51]. Numerous reports have tested subjects
384 on this paradigm translated for use across species in task variants adapted for mice, rats, monkeys, and
385 humans [41, 42, 46]. These studies have shed light on the biological and psychological implications of
386 resolving dissociable, evolutionarily conserved decision-making processes. In the offer zone, individuals
387 engage deliberative systems that represent alternating options of competing actions between which one
388 must choose [54, 55]. This has been shown in rodents to derive in part from hippocampal (HPC)-dependent
389 processes [50, 51]. Population level activity of neurons in HPC is capable of decoding multiple, alternating

390 future paths through the offer zone to potential goals in the current vs. next restaurant [58, 64, 66, 67].
391 Similar findings have been observed from fMRI studies in humans tested on a translated version of the
392 Restaurant Row task [45]. Default mode network activation patterns can decode competing future options
393 during offer zone deliberation, but seldom do such representations include past events or previous
394 restaurants [2, 68]. Decisions in the wait zone on the other hand are much less understood. The HPC has
395 been implicated in wait zone decisions as well: it switches oscillatory activity from a predominately theta-
396 driven state sensitive to the cued offer costs in the offer zone [54] instead to an increase in sharp wave
397 ripple activity sensitive to time spent waiting in the wait zone [55]. Further, wait zone decision periods also
398 depend on HPC synchrony with the mPFC [54, 55]. Recordings in rodents from the mPFC on Restaurant
399 Row surprisingly found no evidence of encoding of the cued offer costs when animals were in the offer zone
400 [52]. However, once in the wait zone, mPFC neurons strongly represented offer value independent of time
401 spent waiting and could predict whether or not the trial would terminate in a quit [52]. Within the mPFC,
402 pairs of neurons also drastically changed excitation-inhibition balance specifically when animals were in the
403 wait zone [69]. Taken together, these findings indicate a qualitative shift in mental state upon transition from
404 the offer zone to the wait zone that recruits the mPFC exclusively during change-of-mind decisions.
405
406 This study represents the first analysis of females in the Restaurant Row task. Nearly all of the sex
407 differences captured here, including those altered by mPFC LINC00473 expression, are restricted to wait
408 zone and not offer zone behaviors. Furthermore, sex differences not only persist but are even exaggerated
409 when access to task-relevant cost information is restricted in the wait zone during change-of-mind
410 decisions. We showed recently that LINC00473 expression diminishes spontaneous excitatory post-
411 synaptic current frequency and amplitude in excitatory mPFC pyramidal neurons of female mice, with no
412 effect seen in males [19]. Chemogenetic inactivation of the mPFC during Restaurant Row diminishes wait
413 zone quit decisions [53-55]. Optogenetic induction of long-term depotentiation in excitatory mPFC neurons
414 that project to the nucleus accumbens (NAc) [50], where negative deflections in dopamine signals have
415 been found to causally precede quit choices on Restaurant Row [70], selectively decreases quitting
416 behavior for several days without altering offer zone behavior [50]. Outside of Restaurant Row, intracranial
417 optogenetic excitatory self-stimulation of mPFC terminals in the NAc can be reinforcing while also promoting

418 enter-then-quitting behavior [71]. These converging findings suggest that LINC00473 expression is likely
419 mediating sex-dependent effects on change-of-mind decisions by at least in part dampening and
420 restructuring mPFC activity. How these alterations in change-of-mind decisions could relate to mPFC
421 LINC00473's known role in enhancing resilience to stress in a sex-dependent manner will help bridge
422 interpretations between molecular drivers of stress responses and the behavioral computations associated
423 with susceptibility vs. resilience to stress in males and females.
424
425 Recent transcriptomic analyses of human postmortem mPFC obtained from individuals diagnosed
426 with major depressive disorder revealed a female-specific decrease in LINC00473 expression in the mPFC
427 [19]. While LINC00473 is not normally expressed in rodents – it arose in the primate lineage – expressing
428 LINC00473 in mouse mPFC neurons demonstrated pro-resilient effects in females, but not males,
429 protecting against several depressive-like phenotypes in simple behavioral tests after exposure to chronic
430 social defeat or variable stress [19]. LINC00473 expression, which predominates in pyramidal neurons in
431 human mPFC [19], has been shown to be regulated by conserved Ca^{2+}/calmodulin signaling pathways and
432 is likely induced by cAMP response element-binding protein (CREB) [19-21, 23]. CREB has long been
433 studied based on more traditional candidate gene approaches and shown to regulate numerous other
434 genes involved in neuronal excitability and synaptic plasticity as well as stress sensitivity [72-77]. Like
435 LINC00473, CREB function in the mPFC has been implicated in promoting resilience to stress, however,
436 unlike LINC00473, this has been shown to be true for both males and females [19, 78]. These reports
437 suggest either that there must be some divergence of intracellular CREB-LINC00473-interacting molecular
438 pathways between sexes conferring differential sensitivities to stress, or that prior studies were limited in
439 their ability to resolve more nuanced sex differences at the behavioral level.
440
441 We recently characterized the impact of chronic social defeat stress on Restaurant Row behavior
442 in male mice, in tandem with disruptions of CREB function in mPFC [33, 48, 79]. First, we found that male
443 mice were required to progress through worsening economic challenges in order to extract any group
444 differences in foraging profiles [33]. This is consistent with results presented here that emphasize the
445 importance of considering the environmental demand and stressors of a task necessary to unmask disease-

446 relevant phenotypes. Second, we found that stress-resilient mice – defined by a simple social interaction
447 screening test measured outside of the Restaurant Row task – mounted the most robust behavioral
448 activation in response to the transition into the 1-30 s reward-scarce environment in efforts to recover and
449 maintain food security despite budget constraints, similar to LINC00473-expressing female mice as shown
450 here [33]. Third, without grossly altering decision-making thresholds, we found that stress-susceptible male
451 mice demonstrated increased regret-related sensitivity to type 1 scenarios (economically risky decisions to
452 skip, followed by poor outcomes), a phenotype no group demonstrated in the present study [48].
453 Additionally, stress-susceptible mice demonstrated diminished regret-related sensitivity to type 2 scenarios
454 (change-of-mind decisions) compared to stress-resilient individuals who instead displayed enhanced
455 change-of-mind sensitivity to both regret and sunk costs related to quitting behavior [48]. Interestingly, in
456 the present study, this constellation of differences was only apparent among the GFP-expressing and
457 LINC00473-expressing females, respectively, suggesting that females at baseline have a decision-making
458 vulnerability specifically in change-of-mind choice processes that is restored to male levels by LINC00473
459 expression in mPFC. In our earlier study, knocking down CREB function had multifactorial effects
460 depending on the neuroeconomic valuation algorithm in question, the brain region targeted (mPFC vs.
461 NAc), and whether or not animals were stress-naïve at baseline vs. exposed to subsequent stress [48].
462 CREB function in the mPFC was required to maintain suppression of regret-related sensitivity to type 1
463 scenarios and, when knocked down, rendered only type 2 scenarios sensitive to subsequent stress – a
464 response profile distinct from CREB function in the NAc where it is known to drive stress susceptibility [48,
465 72, 80, 81]. These data shed light on a divergence between CREB and LINC00473 in mediating dissociable
466 aspects of counterfactual thinking that could independently contribute to the affective toll of past mistakes
467 and one's overall mood burden. These data also point to which consequence of changes in counterfactual
468 sensitivity (i.e., resisting an increase in type 1 or promoting type 2) could be uniquely ascribed to the pro-
469 resilient features of mPFC LINC00473 expression. While these prior studies were conducted in males [33,
470 48, 79], they highlight multiple dimensions with which to consider how information integrates across
471 fundamentally distinct choice processes in order to ultimately precipitate sex-dependent behavioral
472 phenotypes related to one's stress vulnerability.
473

474 LINC00473's sex-dependent effects on behavior have only been causally tested in the mPFC to
475 date [19]. Although postmortem human tissue studies implicate mPFC as a top region to investigate [19],
476 understanding LINC00473's role in other regions, especially in how it may be interacting with other key
477 molecular players such as CREB in the NAc [23, 72, 73], will be critically important in future studies to
478 elucidate how information processing integrates across neural networks. For instance, LINC00473 has
479 been shown to increase cellular excitability in cultured HPC neurons [23], contrary to its effects in mPFC
480 [19]. Future decision-making studies should combine experiments of LINC00473 manipulations with
481 exposure to other stressors, beyond the economic challenges tested in the present study, such as chronic
482 social defeat or variable stress as well as metabolic effects of these stressors to explore compounding
483 effects on decision-making [19]. Further, more work needs to be done toward investigating the role of
484 gonadal steroid hormones, sex chromosomes, and sex-dependent noncoding RNAs in mediating aspects
485 of the reported sex differences. As just one example, CREB function has been shown to fluctuate with
486 estrus cycle [82-86]. Additionally, given previous reports that LINC00473 expression in mPFC of stress-
487 naïve male mice can induce behavioral changes in certain simpler assays (i.e., marble burying) [19], it
488 would be fruitful to explore in future work how Restaurant Row decision-making profiles could potentially
489 relate to individual differences in other traits outside of the task itself (e.g., anxiety-related behavior
490 measured on independent tests). Lastly, it is critically important to consider how the decision-making
491 processes as measured here could relate directly to and drive information processing during the expression
492 of one's symptomology itself (e.g., underlying the choices leading to anhedonia or social avoidance related
493 behaviors themselves) as opposed to occupying a more general role as a trait of the individual.
494
495 Taken together, we discovered robust sex differences in the overall contrast of how an individual
496 decides to change one's mind. This is conceptualized as how dynamic a value representation can be when
497 deciding to quit an ongoing endeavor and the strength with which quitting behavior can influence the
498 psychology of multiple cognitive processes. We characterized this as both the steepness of a tipping point
499 during change-of-mind decisions to either stay or quit and the weight with which such events can be carried
500 into future choices. We found that this lability depends on individual differences in one's subjective value,
501 on the state of the environment in the form of how scarce reward availability and access to information

502 might be, and is uniquely enhanced by LINC00473 expression in the mPFC of females. Counterfactual
503 thinking during change-of-mind decisions can elicit “should not have done that” mental representations that
504 map hypothetical outcomes onto alternative actions that could have been selected instead. Even if change-
505 of-mind decisions are an unpleasant experience or evoke to some degree a form of cognitive dissonance,
506 enhancing the sharpness and salience of this process could increase attention paid toward realized losses,
507 can possess utility for fictive learning, and collectively may be a sex-dependent feature of stress resilience
508 altering the lens through which individuals process their prior mistakes.

509 **Figure Captions:**

510

511 **Fig. 1 | Male and female mice acquire the Restaurant Row task. a** Experimental timeline. 40 C57BL/6J
512 mice (20 male, 20 female) underwent stereotaxic surgery, half of each sex receiving AAV-LINC00473 or
513 AAV-GFP viruses injected bilaterally in the mPFC. Mice were allowed to recover before beginning
514 longitudinal testing on the Restaurant Row task for 45 consecutive days. Dashed box indicates time period
515 relevant for this figure: week 1 of behavioral testing. **b** Task schematic. Mice were allotted 30 min daily to
516 invest time foraging for their primary source of food in a self-paced manner. Costs to obtain rewards were
517 in the form of delays mice would have to wait near feeder sites. Mice were required to run in a
518 counterclockwise direction encountering offers for different flavors at each "restaurant" in serial order. Each
519 restaurant, separated by hallways, was divided into a T-shaped "offer zone" choice point and a separate
520 "wait zone" that housed the pellet dispenser. Upon offer zone entry from the correct heading direction, a
521 tone sounded whose pitch indicated the delay mice would have to wait if accepting the offer by entering the
522 wait zone. If entered, tone pitch descended in the wait zone, cuing the indicated delay. Each trial terminated
523 if mice skipped in the offer zone, quit during the countdown in the wait zone, or earned a reward, after which
524 animals were required to proceed to the next restaurant. **c-f** Simple behavioral metrics across the first week
525 of testing during which all offers were 1 s only (lowest pitch, 4 kHz): (c) total distance traveled, (d) laps run
526 in the correct direction, (e) total rewards earned, (f) earnings split by flavors ranked from least to most
527 preferred by summing each day's end-of-session totals in each restaurant. No effect of sex or LINC00473
528 expression was grossly apparent in these initial metrics. Error bars represent ±1 SEM.

529

530 **Fig. 2 | LINC00473 expression in mPFC alters value-dependent, task-driven conditioned place**
531 **preference behavior in females. a** Experimental timeline. Dashed box indicates time period relevant for
532 this figure: two special testing days marked with cyan arrows. **b** Experimental design. Animals were placed
533 in the arena free to roam for 20 min on day 0 and day 8 of the experimental timeline but with no active task
534 to obtain pre-task baseline and post-task experience-related exploratory behavior. **c** Total number of entries
535 and total time spent in the wait zone, aggregated in all restaurants. **d-e** Representative video tracking data
536 from an example mouse [GFP-treated female] recorded during the pre (day 0) and post (day 8) tests. (d)

537 Track plots displaying body position when traveling between restaurants (gray) and when in the wait zone
538 of each restaurant (colored). (e) Occupancy heat maps of the same example mouse in (d). The change in
539 entries into and time spent in each restaurant's wait zone can be calculated as a delta score (post minus
540 pre). **f-g** Delta scores in change of (f) total entries and (g) total time comparing post (day 8) minus pre (day
541 0) time points split by restaurants ranked according to rewards earned on the active task on day 7. Only
542 the most preferred (1st) and least preferred (4th, faint) restaurants are depicted here (see **Supplementary**
543 **Fig. 3** for full dataset and replication cohort). Horizontal dashed gray line indicates delta score of 0.
544 LINC00473 expression in mPFC abolished CPP behavior in most preferred restaurants only in females and
545 only in the time but not entry domain. *Represent significant sex differences. Error bars represent ±1 SEM.
546
547 **Fig. 3 | Escalating reward scarcity unmasks sex-dependent effects of LINC00473 expression in**
548 **mPFC on complex foraging profiles. a** Experimental timeline. Dashed box indicates time period relevant
549 for this figure: the entire 45-day Restaurant Row paradigm. **b** Total rewards earned (black) and laps run in
550 the correct direction (gray). All 40 mice collapsed. Visual guidance color bars along the x-axis reflect the
551 experimental schedules of the change the distribution of offer costs illustrated in the timeline in (a). Vertical
552 dashed green-yellow-red lines indicate the transition points of the stepwise schedule of and are re-used
553 throughout all other figures as a visual aid. Inset depicts "hysteresis" plot of laps against earns (epochs of
554 days are color-coded). **c** Rewards earned split by flavors ranked from most preferred (1st) to least preferred
555 (4th, faint). All 40 mice collapsed. **d** Change in rewards earned in each restaurant comparing two days at
556 various color-coded transition points (delta scores calculated by subtracting the following: i, day 8-7
557 (yellow); ii, day 13-12 (orange); iii, day 18-17 (red); iv, day 45-18 (purple). All 40 mice collapsed (see
558 **Supplementary Fig. 4** for comparison between groups). **e** The portion of total session time engaged in one
559 of the four major choice behaviors: offer zone – enter (green) or skip (red); wait zone – quit (magenta) or
560 earn (blue). Rings split restaurants ranked from most preferred (1st, inner ring) to least preferred (4th, outer
561 ring). Each of the 5 pie charts represent data from each stage of testing, with the early and late epochs
562 during the 1-30 s offer range extracted from the first 5 and last 5 days of that period. **f** Laps run in the correct
563 direction split by sex and treatment groups. **g** Proportion of enter decisions that terminated in a quit outcome
564 once in the wait zone. LINC00473 expression in mPFC drove females to run more laps in response to a

worsening economic landscape and quit more frequently. *Represent significant sex differences. Shading / error bars represent ±1 SEM.

Fig. 4 | Females demonstrate unique neuroeconomic decision-making policies during change-of-mind choices. a Experimental timeline. Dashed box indicates time period relevant for this figure: the entire 45-day Restaurant Row paradigm. **b** Example behavior from a single mouse early or late during the final 1-30 s testing epoch (red portion of the experimental timeline). Data depict offer zone choice outcomes on the y-axis (enter vs. skip) as a function of the randomly presented cued offer cost (tone pitch) on the x-axis in each restaurant (dots represent individual trial choice outcomes). Quit outcomes in the wait zone are indicated in black dots. **c** Aggregate example summary choice data from all 40 mice early or late during the final 1-30 s testing epoch. Data depict separate offer zone or wait zone summary probability of choice outcome. Horizontal dashed gray line indicates chance at 0.5. Mirror curves for skip and quit (1-probabilities) are intended to highlight cross over points that approximate threshold fits. **d** Thresholds or indifference points of willingness to accept offers in the offer zone or earn offers in the wait zone. Inset depicts an example session from a single mouse in one restaurant where vertical solid green or blue lines illustrate the inflection of Heaviside-step regression fits to choice outcomes in each zone as a function of starting offer costs. All 40 mice collapsed. Inset depicts “hysteresis” plot of offer zone against wait zone thresholds (epochs of days are color-coded). **e** Offer zone thresholds (top) and wait zone thresholds (bottom) split by sex and treatment groups. GFP groups in faint dashed lines. **f** Thresholds from (e) extracted from early and late 1-30 s epoch (red). GFP groups in dashed lines. **g-i** Economic analysis of how well offer zone and wait zone decision policies during the 1-30 s epoch approximate subjective value yield as determined from individual differences in earnings by flavor acquired during the low-cost environment earlier in testing (day 7) when all rewards cost only 1 s. This is compared against theoretical decision policies that maximize total food intake during the 1-30 s epoch irrespective of flavor. See **Methods** and **Supplementary Fig. 6** for a full explanation of this analysis. (g) Individual differences in (top) the standard deviation of rewards earned across flavors on day 7, (middle) total rewards earned on day 7, and (bottom) earns split by restaurant coded in color (flavor: chocolate-brown, banana-yellow, grape-purple, plain-cyan) and size (reward count) on day 7. All data in (g) is sorted by stdev data in (top). Small colored

boxes along the x-axis indicate sex (male-blue, female-red) and treatment groups (LINC-dark, GFP-light). **h** Example data from a single mouse on day 7 showing value ratios among earns between restaurants relative to the least preferred flavor (faint). **i** Data from (g-h) used in a computational modeling analysis to calculate the Euclidean distance between observed decision policies each day from days 18-45 (cool to warm colors, each dot indicates group average per day) to theoretical policies that could achieve either maximal food (x-axis) or maximal subjective value (y-axis) for offer zone and wait zone thresholds. Inset diagonal lines indicate reference point for the 1:1 unity line. Prominent sex difference, without apparent effect of LINC00473 expression in mPFC, in present in wait zone but not offer zone economic decision policies. *Represent significant sex differences. Shading / error bars represent ±1 SEM.

Fig. 5 | LINC00473 expression in mPFC enhances change-of-mind contrast via sensitivity to sunk costs and action-specific regret. a Distribution of quit trials as a function of offer value (x-axis) or value left at the moment of quitting (y-axis) defined relative to one's wait zone threshold (origin vertical and horizontal dashed blue lines). Data split by restaurants ranked from least to most preferred. All 40 mice collapsed. Data extracted from the entire 1-30 s epoch. **b** Average value left at the moment of quitting split by sex and treatment groups. Horizontal dashed gray line indicates 0 value left (or wait zone threshold). **c** Three categories of quit events based on offer value and value left terms. The green quadrant ($V_o<0$ & $V_L<0$) represent the most efficient quit decisions from economically disadvantageous offers. **d** Counts of total number of quit events aggregated across all restaurants from each economic quit category described in (c). **e** Counts of total number of quit events from each economic quit category in (d) split by restaurants ranked from least (4th) to most preferred (1st) extracted from the entire 1-30 s epoch (red). **f-h** Sunk cost analysis of staying behavior in the wait zone, demonstrated using all 40 mice. (f) The likelihood of staying in the wait zone and earning a reward (e.g., not quit) is plotted as a function of time left in the countdown along the x-axis and time already spent waiting orthogonally in color. Note the black 0 s time spent curve represents animals having just entered the wait zone from the offer zone. Inset vertical dashed gray line illustrates an example analysis point comparing three sunk cost conditions originating from different starting offers but matched at 10 s left. Data from (f) dimensioned reduced in (g) collapsing across time left, highlighting the grand mean of each time spent sunk cost condition (color and x-axis). Insets in (g) depict

621 data from curves in (f) are collapsed into the observed (sunk condition) and control (0 s condition) lines.
622 Difference between curves in (g) are plotted in (h) in order to summarize the envelope of the overall effect
623 of time already spent on escalating the commitment of staying in the wait zone. Horizontal dashed line
624 represents delta score of 0. **i** Sensitivity to sunk costs plotted across the entire Restaurant Row paradigm
625 where the delta curve in (h) is plotted as vertical slices in (i) with time already spent along the y-axis and
626 heatmap representing delta score magnitude. **j-k** Regret-related sequence analyses comparing trial pairs
627 between (j) type 1 scenarios and (k) type 2 scenarios each. Read out trials captures a change in behavior
628 depending on choice history of distinct economic violations (black) compared to non-violations (gray) on
629 trial t-1. Read out trials report delta scores in likelihood change of entering by subtracting choice outcomes
630 between violation-nonviolation sequences. Horizontal dashed gray line indicates delta score of 0. See
631 **Methods** for a full explanation of these analyses. Prominent sex-dependent effect revealed by LINC00473
632 expression in mPFC on change-of-mind related sunk costs (enhanced in females) and regret sensitivity
633 (type 2: enhanced in females). ***** in (b-i) represent significant sex differences. * in (j-k) represent delta score
634 significantly different from 0. Shading / error bars represent ±1 SEM.
635
636 **Fig. 6 | Sex- and LINC00473-dependent wait zone behaviors are differentially modulated by access**
637 **to task information. a** Informational manipulation schematic: (left) standard Restaurant Row task followed
638 by (right) two days of tones silenced only in the wait zone, but not offer zone (remains audible as before).
639 **b** Total number of laps run in the correct direction (top) and total pellets earned aggregated among
640 restaurants (bottom) across the audible and silent wait zone task conditions (x-axis). **c** Rewards earned in
641 each restaurant ranked from least (4th) to most preferred (1st) across the audible (black) and silent wait zone
642 (gray) task conditions. **d** Overall offer zone choice probabilities to make enter decisions as a function of
643 audible cued offer costs collapsed across all flavors to illustrate no effect of task condition on auditory
644 discriminatory behaviors. Horizontal dashed line indicates change at 0.5. **e** Wait zone thresholds in each
645 restaurant across task conditions. **f** Latency to quit reaction times once in the wait zone in each restaurant
646 across task conditions. **g** Sensitivity to sunk costs in the wait zone depicted here only in the silent condition
647 as a function of time already spent (x-axis). Y-axis reflects delta earn probabilities as depicted in Fig. 5h.
648 Prominent sex-dependent effects of withholding wait zone information on overall task performance

649 (observed in males), wait zone economic decision policies (bidirectional in males, unidirectional in GFP-
650 females, and no effect in LINC00473-females), and sunk cost sensitivity (sex difference revealed for the
651 first time GFP groups unlike in Fig. 5). Horizontal dashed line indicates delta score of 0. ***** in (b-f) represent
652 significant effects of task condition within group. * in (g) represent significant sex differences. Shading /
653 error bars represent ±1 SEM.

Acknowledgments:

We thank members of the labs of Eric Nestler and Scott Russo for helpful discussion and technical assistance. Open-source illustrations obtained from SciDraw (www.scidraw.io), credit Federico Claudi.

Funding:

National Institute of Mental Health grant R01MH051399 (EJN)
National Institute of Mental Health grant R01MH129306 (EJN)
National Institute of Mental Health grant R01MH114882 (SJR)
National Institute of Mental Health grant R01MH127820 (SJR)
National Institute of Mental Health grant R01MH104559 (SJR)
National Institute of Mental Health grant L40MH127601 (BMS)
National Institute of Mental Health training grant R25MH129256 (BMS)
National Institute of Mental Health supplement grant R01MH051399-31S1 (BMS)
Leon Levy Scholarship in Neuroscience, New York Academy of Sciences (BMS)
Burroughs Wellcome Fund Career Award for Medical Scientists (BMS)
Animal Models for the Social Dimensions of Health and Aging Research Network via NIH/NIA R24 AG065172 (BMS)
Brain & Behavior Research Foundation Young Investigator Award 31140 (RDC)

Author contributions:

Conceptualization: RDC, OI, EJN, BMS
Methodology: RDC, OI, BMS
Investigation: RDC, BY, NJ, AA, SK, KG, SA, SJR, EJN, OI, BMS
Data curation: RDC, OI, BMS

682 Formal analysis: BMS

683 Visualization: RDC, OI, BMS

684 Funding acquisition: OI, BMS

685 Supervision: RDC, BMS

686 Writing – original draft: RDC, OI, BMS

687 Writing – review & editing: RDC, BY, NJ, AA, SK, KG, SA, SJR, EJN, OI, BMS

688

689 **Competing interests:**

690

691 Authors declare that they have no competing interests.

692

693 **Data and materials availability:**

694

695 All data and materials used in the analysis are available in the manuscript, materials and methods

696 section, or supplementary information.

697 **Supplementary Figure Captions**

698

699 **Supplementary Fig. 1 | Validation of newly packaged adeno-associated virus expression of**
700 **LINC00473.** Raw qPCR cycle threshold count (ct) obtain from mPFC tissue punches extracted from mice
701 separately transfected with either AAV2-hSyn-GFP (control) or AAV2-hSyn-LINC00473-GFP (treatment).
702 qPCR readouts obtained for expression levels of GFP, HPRT1 (housekeeping), ZFP189 (another known
703 regulator of stress-resilience), and LINC00473. Note similar levels of expression of GFP (t=2.03, p=0.089),
704 HPRT1 (t=0.41, p=0.693), and ZFP189 (t=0.91, p=0.396) between control and treatment viruses. Also note
705 no detectable levels of LINC00473 in mice transfected with the control virus, as this is not endogenously
706 expressed in mice. Dots represent individual samples. Error bars represent ±1 SEM.

707

708 **Supplementary Fig. 2 | Bodyweight measurements.** Percentage of a 2-day average (circled in gray,
709 horizontal dashed line for reference) of baseline body weight obtained 4 days prior (black epoch) to the
710 start of the longitudinal Restaurant Row paradigm. During this period (black epoch), mice were food
711 restricted and fed a limited ration to intentionally decrease weights to approximately 80-85% of baseline
712 that was steadily maintained throughout the remainder of the experiment (days 1-45, see **Fig. 1** for an
713 explanation of the color-coded epochs of testing across the paradigm). These body weights reflect the
714 measurements immediately before task performance on each day of testing. There were no differences in
715 percentage baseline bodyweight between groups (virus: F=0.292, p=0.593; sex: F=0.118, p=0.733).
716 Shaded area represents ±1 SEM.

717

718 **Supplementary Fig. 3 | Replication cohort of two different virus titers on sex-specific Restaurant**
719 **Row conditioned place preference (CPP) findings.** Animals were placed in the arena free to roam for
720 20 min on day 0 and day 8 of the experimental timeline but with no active task to obtain pre-task baseline
721 and post-task experience-related exploratory behavior (see **Fig. 2**). **a** Total number of entries and total time
722 spent in the wait zone, aggregated in all restaurants. Depicting findings from independent cohorts: surgeries
723 and behavioral experiments were carried out across separate calendar months and using different virus
724 titers. **b** Delta scores in change of entries and time comparing post (day 8) minus pre (day 0) time points
725 split by restaurants ranked according to rewards earned on the active task on day 7. **c** Data from (b, only

726 1st and 4th ranking restaurants) replotted with number of rewards earned on day 7 on the x-axis. Horizontal
727 dashed gray line indicates delta score of 0. LINC00473 expression in mPFC abolished CPP behavior in
728 most preferred restaurants only in females and only in the time but not entry domain, replicated in both
729 cohorts. +Sign-test on delta score of time: low virus cohort: male GFP: (t=2.142, p<0.05); female GFP:
730 (t=4.424, p<0.01); female LNC: (t=0.04, p=0.516); high virus cohort: male GFP: (t=8.681, p<0.0001); male
731 LINC: (t=5.087, p<0.001); female GFP: (t=7.157, p<0.0001); female LNC: (t=0.962, p=0.181). +Sign-test
732 on delta score of entries: low virus cohort: male GFP: (t=0.955, p=0.197); female GFP: (t=3.155, p<0.05);
733 female LNC: (t=3.766, p<0.01); high virus cohort: male GFP: (t=3.520, p<0.01); male LINC: (t=2.493,
734 p<0.05); female GFP: (t=3.236, p<0.01); female LNC: (t=2.355, p<0.05). Error bars represent ±1 SEM.
735
736 **Supplementary Fig. 4 | Basic Restaurant Row laps and earnings metrics across testing. a** Overall
737 sex difference comparisons between males and females (collapsing across GFP and LINC00473 virus
738 treatment within each sex). Average number of laps run in the correct direction (sex*day: F=78.040,
739 p<0.0001), total rewards earned (sex*day: F=1.331, p=0.249), ratio of earns / laps (sex*day: F=28.155,
740 p<0.0001), and standard deviation of earns among flavors (sex*day: F=13.014, p<0.001). **b** Data from (a)
741 split by GFP and LINC groups: laps (sex*virus*day: F=0.008, p=0.927), total earns (sex*virus*day: F=7.470,
742 p<0.01), ratio of earns / laps (sex*virus*day: F=1.130, p=0.288), standard deviation of earns by flavor
743 (sex*virus*day: F=15.486, p<0.0001). Statistical tests from (a) and (b) were performed on the entire
744 experimental timeline (days 1-45). **c** Data from main Fig. 3d split by sex and virus groups depicting change
745 in rewards earned in each restaurant comparing two days at each color-coded transition point. Delta scores
746 calculated by subtracting the following: i, day 8-7 (yellow, rank: F=1.361, p=0.259; sex*virus: F=0.017,
747 p=0.897); ii, day 13-12 (orange, rank: F=1.123, p=0.343; sex*virus: F=0.086, p=0.769); iii, day 18-17 (red,
748 rank: F=18.116, p<0.0001; sex*virus: F=0.076, p=0.783); iv, day 45-18 (purple, rank: F=0.603, p=0.614;
749 sex*virus: F=0.375, p=0.542). Shaded area and error bars represent ±1 SEM.
750
751 **Supplementary Fig. 5 | Restaurant Row choice metrics split by flavor ranking across testing. a**
752 Average number of enter decisions made in the offer zone split by sex and virus treatment groups as well
753 as the 4th and 1st ranking restaurant (sex*rank*day: F=16.043, p<0.0001; sex*virus*rank*day: F=3.967,

754 $p<0.01$). **b** Number of skip decisions made in the offer zone (sex*rank*day: $F=9.894$, $p<0.0001$;
755 sex*virus*rank*day: $F=2.617$, $p<0.05$). **c** Offer zone reaction time before making an enter or skip decision
756 calculated from offer zone entry (tone onset) to either a right turn into the wait zone (enter) or a left turn into
757 the hallway (skip) (sex*rank*day: $F=0.325$, $p=0.808$; sex*virus*rank*day: $F=2.186$, $p=0.087$). **d** Number of
758 quit decisions made in the wait zone during a countdown (sex*rank*day: $F=11.725$, $p<0.0001$;
759 sex*virus*rank*day: $F=1.216$, $p=0.302$). **e** The probability of quitting in the wait zone given the animal
760 entered (sex*rank*day: $F=4.145$, $p<0.01$; sex*virus*rank*day: $F=0.463$, $p=0.708$). This normalizes the
761 likelihood of quitting to enter frequency. **f** Wait zone latency to quit reaction time from countdown onset
762 (wait zone entry) until mice leave the wait zone prematurely (sex*rank*day: $F=1.427$, $p=0.233$;
763 sex*virus*rank*day: $F=3.160$, $p<0.05$). Statistical tests here were performed on the entire experimental
764 timeline (days 1-45). Shaded area represents ±1 SEM.
765
766 **Supplementary Fig. 6 | Longitudinal economic analysis of decision policy optimization for food**
767 **security vs. subjective value.** Analysis underlying data from main Fig. 4g-i derived from Durand-de Cuttoli
768 et al 2023 *Biological Psychiatry* [33]. **a** Computer Restaurant Row simulation of total number of pellets
769 earned. The ideal threshold required to obtain the theoretical maximum number of pellets when ignoring
770 flavor preferences was empirically determined to be 10 s. **b** Relative ratio of earns among restaurants for
771 an example mouse on day 7 between the flavor rankings (i.e., this mouse had a 3.7 : 2.1 : 1.4 : 1 ratio of
772 earns across flavors capturing a summary of idealized relative subjective value for this mouse when all
773 offers were 1 s only). **c** Two intersecting planes of decision policies that yield varying amounts of theoretical
774 value either for maximal food intake (as determined by computer simulations, brown plane) or subjective
775 value (as determined by multiplying day 7 preference ratios on a mouse-by-mouse basis, pink plane) when
776 in a reward-scarce environment (1 to 30 s offers). Here, only two decision policy dimensions (least preferred
777 and most preferred restaurants) of the four dimensions (all four ranked restaurants) are displayed. Both
778 planes are normalized to each's min and max values for the purpose of plotting both in the same space
779 while preserving the threshold coordinate locations that achieve either theoretical maximum (brown
780 [location always fixed at threshold coordinates of 10 s] or pink beacons [location of discovered threshold
781 coordinates that vary from mouse-to-mouse]). Actual observed daily decision policies represented by the

782 cyan beacon wander throughout this space from day 18 to 45 in a reward-scarce environment. Trajectories
783 projected to the floor of this display trace out individual mouse decision policy paths. Example coordinates
784 of brown, pink, and cyan beacons illustrated as dots on the x and y axes. Euclidean distance from cyan
785 coordinates to either brown or pink coordinates were calculated (question mark symbols). **d** Euclidean
786 distances from observed decision policies in the offer zone (left) or wait zone (right) to either food (brown)
787 or preference (magenta) theoretical maximum across testing in a reward-scarce environment split by GFP
788 (top) and LINC (bottom) groups and sex. Offer zone: food distance: day: F=49.362, p<0.0001; sex: F=1.115,
789 p=0.298; virus: F=0.008, p=0.929; value distance: day: F=42.042, p<0.0001, sex: F=1.546, p=0.221; virus:
790 F=0.001, p=0.989; Wait zone: food distance: day: F=16.774, p<0.001, sex: F=13.796, p<0.001; virus:
791 F=0.598, p=0.445; value distance: day: F=38.046, p<0.0001, sex: F=18.034, p<0.0001; virus: F=0.261,
792 p=0.613. Shaded area represents ±1 SEM.
793
794 **Supplementary Fig. 7 | Sensitivity to sunk costs analysis during the 1-15 s testing epoch.** Mice do
795 not display sensitivity to sunk costs during days 13-17 in a relatively reward rich environment compared to
796 days 18+ (when offers range 1-30 s, as in main Fig. 5). **a-c** Sunk cost analysis of staying behavior in the
797 wait zone, demonstrated using all 40 mice. (f) The likelihood of staying in the wait zone and earning a
798 reward (e.g., not quit) is plotted as a function of time left in the countdown along the x-axis and time already
799 spent waiting orthogonally in color. Note the black 0 s time spent curve represents animals having just
800 entered the wait zone from the offer zone. Inset vertical dashed gray line illustrates an example analysis
801 point comparing three sunk cost conditions originating from different starting offers but matched at 10 s left.
802 Data from (a) dimensioned reduced in (b) collapsing across time left, highlighting the grand mean of each
803 time spent sunk cost condition (color and x-axis). Difference between curves in (b) are plotted in (c) in order
804 to summarize the envelope of the overall effect of time already spent on escalating the commitment of
805 staying in the wait zone. Horizontal dashed line represents delta score of 0. **d** Data in (c) split by sex and
806 virus treatment groups depicting no effect of time spent during the countdown in the wait zone on changing
807 the probability of quitting vs. staying to earn a reward (time spent: F=0.522, p=0.470; sex*virus*time spent:
808 F=0.809, p=0.369). **e** To compare to time spent waiting in the wait zone, data here depict a different type
809 of time spent on the task: time spent in the offer zone prior to accepting an offer and entering the wait zone

810 does not influence the probability of quitting vs. staying to earn a reward once in the wait zone (time spent
811 in offer zone: F=1.574, p=0.210; sex*virus*time spent: F=0.916, p=0.339). These data are from the 1-30 s
812 reward-scarce epoch (days 18-45) to demonstrate the unique value of time spent waiting in the wait zone
813 uniquely conferring sunk cost sensitivity. Error bars represent ±1 SEM.
814
815 **Supplementary Fig. 8 | Full set of task information manipulations on Restaurant Row. a** After day 45,
816 mice were challenged with special probe days on three different task informational manipulations each for
817 2 days. Manipulations took the form of silencing and withholding tone presentation either in the offer zone,
818 wait zone, or both: (i) silent offer zone but audible wait zone [days 46-47], (ii) audible offer zone but silent
819 wait zone [days 48-49], and (iii) silent offer zone and silent wait zone [days 50-51]. **b** Offer zone choice
820 probability to enter as a function of offer cost split by restaurants ranked from least (4th) to most (1st)
821 preferred separating sex and virus treatment groups (rows) across the 4 different task information
822 conditions (columns). **c** Data in (b) collapsed across all four restaurants showing summary enter
823 probabilities as a function of offer cost. Note that enter probabilities are largely unaffected when the offer
824 zone tones are audible comparing baseline (black, regular task) to silent wait zone (blue) conditions,
825 however, as intended, offer zone choice probabilities change into a flat horizontal line in both the silent offer
826 zone (green) and silent task (gray) conditions, as animals do not have any tone information in the offer zone
827 during these conditions (audible task: offer: F=2017.115, p<0.0001; sex*virus*offer: F=1.912, p=0.167;
828 silent offer zone task: offer: F=1.783, p=0.182; sex*virus*offer: F=0.227, p=0.634; silent wait zone task:
829 offer: F=1004.552, p<0.0001; sex*virus*offer: F=0.147, p=0.702; fully silent task: offer: F=0.723, p=0.395;
830 sex*virus*offer: F=1.723, p=0.190). **d** Wait zone thresholds plotted as a relative fold change comparing
831 each condition to the regular task audible baseline separated across the three information manipulations
832 (silent offer zone, left, green; silent wait zone, middle, blue; silent task, right, gray) split by restaurants
833 ranked from least (4th) to most (1st) preferred, sex, and virus treatment groups. Note the difference in
834 patterns in changes in wait zone thresholds across restaurants between sex/virus groups and across task
835 information manipulation conditions. Sign tests: silent offer zone: male GFP: least preferred: t=+1.365,
836 p=0.103; most preferred: t=+2.639, p<0.05; male LNC: least preferred: t=+2.699, p<0.05; most preferred:
837 t=+1.538, p=0.079; female GFP: least preferred: t=+3.638, p<0.01; most preferred: t=+0.360, p=0.363;

838 female LNC: least preferred: t=+2.125, p=<0.05; most preferred: t=+0.188, p=0.427; silent wait zone: male
839 GFP: least preferred: t=-2.684, p<0.05; most preferred: t=+3.191, p<0.01; male LNC: least preferred: t=-
840 2.624, p<0.05; most preferred: t=+2.685, p<0.05; female GFP: least preferred: t=-4.733, p<0.001; most
841 preferred: t=+1.325, p=0.109; female LNC: least preferred: t=-0.411, p=0.345; most preferred: t=+0.886,
842 p=0.199; silent task: male GFP: least preferred: t=-0.358, p=0.364; most preferred: t=+5.554, p<0.001; male
843 LNC: least preferred: t=+0.794, p=0.225; most preferred: t=+3.049, p<0.001; female GFP: least preferred:
844 t=-3.584, p<0.01; most preferred: t=+2.345, p<0.05; female LNC: least preferred: t=-1.009, p=0.170; most
845 preferred: t=+1.671, p=0.064. Shaded area and error bars represent ±1 SEM.

846 **Methods**

847 *Subjects:* Adult male and female C57BL/6J mice (Jackson, 10wks, n=40) were used. Mice
848 were individually housed and maintained on a 12-hr light/dark cycle with ad libitum water, only
849 food-restricted during Restaurant Row testing, conducted during their light phase. Experiments
850 were approved by the Mount Sinai Institutional Animal Care and Use Committee (IACUC; protocol
851 number LA12-00051) and adhered to the National Institutes of Health (NIH) guidelines.

852

853 *Viral constructs:* To achieve long-term neuronal expression of LINC00473, it was
854 subcloned into an AAV plasmid with human synapsin promoter (hSyn) driving gene expression.
855 LINC00473 transcript variant 1, (NR_026860.1 /AK289375) of 1821bp length was subcloned from
856 p1005+ HSV vector (PMID: 32304628) into pAAV-hSyn-eGFP-hSny plasmid (PMID: 36449610)
857 using blunt ligation into a PMEI and EcoRV restriction sites following the second hSyn promoter.
858 The orientation and sequence were validated using Sanger sequencing. Empty plasmid
859 expressing eGFP only was used as control. These vectors were used to generate AAV serotype
860 2 at the University of Maryland virus vector core. Viral vector placement and expression were
861 confirmed in vivo by a GFP fluorescent flashlight and qPCR.

862

863 *RNA extraction, RT, and qPCR:* Total RNA was isolated and purified with RNeasy Micro
864 Kit (Qiagen), using QIAzol as a lysis reagent, including DNase treatment. All samples were tested
865 for concentration and purity using a NanoDrop (Thermo Fisher). RNA amount was normalized
866 across samples (400ng), and cDNA was created using iScript (Bio-Rad). Real-time PCR reactions
867 were run in triplicate using PowerUp SYBR Master Mix (Applied Biosystems) in a QuantStudio 7
868 (Thermo Fisher) qPCR machine. Primer sequences: LINC00473: forward:
869 GCATACTTTGGCGGACCTTTT, reverse TGTGCCTCCCTGTGAATTCTC; HPRT1 forward:
870 GCAGTACAGCCCCAAAATGG, reverse: GGTCCTTTTCACCAGCAAGCT; GFP forward:

871 CATGCCCGAAGGCTACGT, reverse CGATGCCCTTCAGCTCGAT. Raw Ct values are
872 presented and not normalized amounts, as LINC00473 is not endogenously expressed in mice.
873
874 *Virus surgery:* Mice were anesthetized by intraperitoneal injection with a mixture of
875 Ketamine HCl (100 mg/kg) and Xylazine (10 mg/kg) and positioned on a stereotaxic instrument
876 (David Kopf Instruments). In the medial prefrontal cortex (mPFC, from bregma with an angle of
877 15 degrees: AP +1.8 mm; ML ±0.75 mm; DV −2.7 mm), 0.7 µL of virus (AAV2-hSyn-GFP or AAV2-
878 hSyn-LINC00473-GFP) was bilaterally infused using 33-Gauge Hamilton needles over 5 min at a
879 rate of 0.1 µL/min, and the needle was left in place for 10-15 min after the injection before
880 retraction. Mice were allotted 2 weeks to recover before beginning food restriction across 3-4 days
881 in preparation for testing on Restaurant Row. An initial virus validation cohort (independent cohort
882 of n=10 mice) was injected with GFP or LINC00473 viruses bilaterally in mPFC at a titer of $1x10^{12}$
883 at. These animals were tested on Restaurant Row for only 1 week (offers remained at 1 s only,
884 first epoch, green) after which they were sacrificed for PCR validation on tissue punches obtained
885 from mPFC. Behavioral data from these animals on the conditioned-place preference probe (days
886 0 and 8) appear in Supplementary Fig. 3. A second replication cohort (n=40 mice) was injected
887 with GFP or LINC00473 viruses bilaterally in mPFC at a titer of $5x10^{12}$ and served as the primary
888 cohort of animals for the main figures that underwent the full 45-day longitudinal behavioral
889 testing.
890
891 *Neuroeconomic Task:* Following surgery, we characterized mice longitudinally in
892 Restaurant Row [5]. On this task, mice had a limited time period each day to forage for food by
893 navigating a maze with four uniquely flavored (chocolate, banana, grape, and plain) and
894 contextualized (horizontal stripes, dots, triangles, vertical stripes) feeding sites, or “restaurants”
895 (Fig. 1b). Animals were allotted 30 min to forage for their primary source of food for the day.
896 Rewards used on this task were obtained from BioServe (20 mg pellets #F007120). These pellets

are full nutrition and not sucrose-only pellets that only differed in flavoring but not nutritional profile (3.6 kcal/gm calories, 59.1% carbohydrate, 18.7% protein, 6.5% ash, 5.6% fat, 4.7% fiber). Choices on this task were interdependent across trials and across days. This makes the task economic in nature, requiring animals to budget their limited time effectively in a self-paced manner in order to earn a sufficient amount of food in a closed-economy system. The cost of earning a reward took place in the form of a delay animals would have to wait cued by the pitch of a tone that sounded upon entry into each restaurant. Each restaurant had a separate offer zone (OZ) and wait zone (WZ). Upon entry into the OZ, a tone (500 ms) sounded whose pitch indicated how long of a delay mice would have to wait in a cued countdown should they enter the WZ. Mice could decide to skip an offer presented in the OZ and proceed down the hallway to the next restaurant. In the OZ, tones repeated every second held at the same pitch to repeatedly cue the offer of the current trial until mice either made a skip or enter decision. If mice decide instead to enter the WZ, this triggered a countdown with descending tone pitch stepping every second until mice either waited out the full delay and earned a food pellet or quit prematurely during the countdown. If mice made a skip or quit decision, the tone terminated, the offer was rescinded, and mice must proceed forward to the next restaurant. Mice quickly learned to only travel in one direction as animals must encounter offers serially navigating the maze in a counterclockwise direction (i.e., nothing happens if mice traverse in the wrong direction other than wasting time). Mice were tested across 45 consecutive days for the main experiment where strategies developed longitudinally as animals learned the structure of the task and the changing economic landscape.

During the first week of testing (block 1, green epoch), all trials consisted of 1 s offers only. 1 s offers were indicated by tones played at the 4,000 Hz pitch. A special probe session was inserted into this timeline immediately before (day 0) and after (day 8) the first week of testing during which mice essentially were allowed to roam the empty maze arena freely without any task components (no tones, no rewards) to examine conditioned place preference behaviors learned

through the natural experience of the first week of the task itself. The remainder of the experimental timeline continued thereafter. During the next 5 days of testing (block 2, yellow epoch), offers ranged from 1 to 5 s (4,000 Hz to 5,548 Hz in 387 Hz steps) randomly selected from a uniform distribution. For instance, if a 4 s offer was selected on a given trial, the tone presented in the OZ would be 5,161 Hz for 500 ms, and this would repeat every second indefinitely until a skip or enter decision was made. If the WZ was entered, using this example trial, this 5,161 Hz tone would step down by 387 Hz every second descending in pitch until earning (with the final tone of 4,000 Hz) or quitting prematurely. Block 3 (5 days, orange epoch) consisted of a 1 to 15 s (4,000–9,418 Hz) range. The fourth and final block (red epoch) consisted of offers ranging from 1 to 30 s (4,000–15,223 Hz) and continued for the remainder of the experiment. This block-wise protocol allowed us to examine how mice initially shaped their behavior as they learned the basic structure of the task as well as how they adjusted their foraging strategies across long timescales (days, weeks, and months) as they transitioned from reward-rich to reward-scarce environments in a stepwise manner. That is, blocks 1-3 are relatively reward rich as costs are generally low delays and rewards are easier to earn compared to block 4 which is relatively reward scarce as there are far more expensive reward offers distributed in the environment for which animals must learn to forage efficiently. The rewards used in this task only differ in flavor for which animals have subjective differences in preferences quantified below. All flavor options become increasingly scarce, equally across the longitudinal paradigm.

Rewards were delivered using a custom-built 3D-printed automated pellet dispenser that was triggered by a computer running the task programmed in ANY-Maze (Stoelting), run under dim lighting. The task was run by video-tracking animal position in real-time where all choice contingencies are determined by the centroid of the animal's body crossing territories in the maze in combination with being required to run in a counterclockwise direction. The key zones in the maze include each restaurant's separate OZ and WZ as well as the hallways in between

949 restaurants (thus, 12 total main zones). 6 key behavioral epochs make up all possible, mutually
950 exclusive behaviors animals could be engaged in while spending their limited time budget. 1)
951 **Enter time**: defined from OZ entry in the correct heading direction (counterclockwise around the
952 maze) triggering tone onset until the animal physically enters right into the WZ triggering tone
953 countdown. 2) **Skip time**: defined from OZ entry in the correct heading direction triggering tone
954 onset until the animal physically exits left into the hallway. 3) **Quit time**: defined from WZ entry
955 and tone countdown onset until the animal physically exits the WZ prematurely before the
956 countdown completes, rescinding the offer and terminating the countdown. 4) **Earn time**: defined
957 from WZ entry and tone countdown onset until the countdown completes and a pellet is delivered.
958 5) **Consumption time**: defined from reward delivery onset until the animal physically leaves the
959 reward site and exits the WZ. 6) **Travel time**: defined from previous trial termination (either from
960 a skip, quit, or consumption event as defined above) and hallway entry until the next trial begins,
961 triggered by OZ entry into the next restaurant.
962
963 Body weight was measured twice daily, immediately before and after testing on the
964 Restaurant Row task.
965
966 *Data analysis*: In addition to simple behavioral metrics like rewards earned, laps run,
967 reaction times as described above, a key neuroeconomic behavioral metric is decision thresholds.
968 This metric approximates indifference points in choices made either in the OZ or WZ as a function
969 of cost and flavor. We measured the inflection point of fitting heaviside step regressions to enter
970 versus skip choices in the OZ or earn versus quit choices in the WZ as a function of cued offer
971 cost in each restaurant. Thresholds determined this way were used for several subsequent
972 analyses, including calculating reward value. The value of an offer can be calculated by
973 subtracting a trial's offer from one's WZ threshold as this reflects the relative cost normalized to
974 each animals' willingness to wait and earn a reward (i.e., offer value <0 indicate offers typically

975 not earned and thus should be skipped in the OZ or quit in the WZ as determined by each animal's
976 subjective flavor-specific decision policy which remained relatively stable across block 4 of
977 testing). Similarly, when quitting in the WZ, the value left at the moment of quitting can be
978 calculated by subtracting the time remaining in that trial's countdown from the WZ threshold (i.e.,
979 value left <0 indicates an amount of time left that is not worth waiting for and should have been
980 quit whereas value left >0 would have been more advantageous to finish waiting at that point
981 instead of quitting). The amount of time spent remaining in the countdown at the moment of
982 quitting relative to what the starting offer was and how much time was spent also served as the
983 basis of our analysis of sensitivity to sunk costs, as previously published in mice, rats, and humas
984 whereby time spent waiting can decrease the probability of quitting independent of time left in the
985 countdown, see Sweis et al *Science* for the development of this analysis [44, 46, 48, 49, 53].
986 Thresholds as well as economic choice history serve as the basis and criteria used in regret-
987 related analysis whereby distinct violation vs. non-violation sequences are compared head-to-
988 head in order to quantify the effects of mistake history on influencing choice behavior on the next
989 trial. See Steiner and Redish 2014 *Nature Neuroscience* [47], Sweis et al 2018 *PloS Biology* [5],
990 and Durand-de Cuttoli 2022 *Science Advances* [48] for the development of these analyses.
991 Thresholds were also used for an analysis we recently developed to capture how mice develop
992 strategies that optimize food yield while also maximizing subjective value, see Durand-de Cuttoli
993 et al 2023 *Biological Psychiatry* [33] for the development of this analysis.
994
995 Data were processed in Matlab with statistical analyses in JMP Pro 17. All data are
996 expressed as mean ± 1 standard error. Statistical significance was assessed using student's t
997 tests, sign tests, and one-way, two-way, three-way, and repeated measures ANOVAs. No data
998 were excluded as outliers.

999 **References**

1000 1. Stone, C., J.B. Mattingley, and D. Rangelov, *On second thoughts: changes of mind in*
1001 *decision-making.* Trends Cogn Sci, 2022. **26**(5): p. 419-431.
1002 2. Liu, X., et al., *Common and distinct networks underlying reward valence and processing*
1003 *stages: a meta-analysis of functional neuroimaging studies.* Neurosci Biobehav Rev,
1004 2011. **35**(5): p. 1219-36.
1005 3. Redish, A.D., *The mind within the brain: How we make decisions and how those decisions*
1006 *go wrong.* 2013: Oxford University Press.
1007 4. McGuire, J.T. and J.W. Kable, *Medial prefrontal cortical activity reflects dynamic re-*
1008 *evaluation during voluntary persistence.* Nat Neurosci, 2015. **18**(5): p. 760-6.
1009 5. Sweis, B.M., M.J. Thomas, and A.D. Redish, *Mice learn to avoid regret.* PLoS Biol, 2018.
1010 **16**(6): p. e2005853.
1011 6. Kirkebøen, G., E. Vasaasen, and K. Halvor Teigen, *Revisions and Regret: The Cost of*
1012 *Changing your Mind.* Journal of Behavioral Decision Making, 2011. **26**(1): p. 1-12.
1013 7. Brenner, C., *The mind in conflict*. 1982, New York: International Universities Press. 266 p.
1014 8. Baumeister, R.F., K.D. Vohs, and D.M. Tice, *The Strength Model of Self-Control.* Current
1015 Directions in Psychological Science, 2016. **16**(6): p. 351-355.
1016 9. American Psychiatric Association. and American Psychiatric Association. DSM-5 Task
1017 Force., *Diagnostic and statistical manual of mental disorders : DSM-5*. 5th ed. 2013,
1018 Washington, D.C.: American Psychiatric Association. xliv, 947 p.
1019 10. Mezo, P.G. and R.M. Baker, *The moderating effects of stress and rumination on*
1020 *depressive symptoms in women and men.* Stress Health, 2012. **28**(4): p. 333-9.
1021 11. Seedat, S., et al., *Cross-National Associations Between Gender and Mental Disorders in*
1022 *the World Health Organization World Mental Health Surveys.* Archives of General
1023 Psychiatry, 2009. **66**(7).

1024 12. Ferrari, A.J., et al., *Burden of depressive disorders by country, sex, age, and year: findings*
1025 *from the global burden of disease study 2010.* PLoS Med, 2013. **10**(11): p. e1001547.
1026 13. Marcus, S.M., et al., *Sex differences in depression symptoms in treatment-seeking adults:*
1027 *confirmatory analyses from the Sequenced Treatment Alternatives to Relieve Depression*
1028 *study.* Compr Psychiatry, 2008. **49**(3): p. 238-46.
1029 14. Silverstein, B., *Gender differences in the prevalence of somatic versus pure depression:*
1030 *a replication.* Am J Psychiatry, 2002. **159**(6): p. 1051-2.
1031 15. Martin, L.A., H.W. Neighbors, and D.M. Griffith, *The experience of symptoms of*
1032 *depression in men vs women: analysis of the National Comorbidity Survey Replication.*
1033 JAMA Psychiatry, 2013. **70**(10): p. 1100-6.
1034 16. Eid, R.S., A.R. Gobinath, and L.A.M. Galea, *Sex differences in depression: Insights from*
1035 *clinical and preclinical studies.* Prog Neurobiol, 2019. **176**: p. 86-102.
1036 17. Akil, H., et al., *Treatment resistant depression: A multi-scale, systems biology approach.*
1037 Neurosci Biobehav Rev, 2018. **84**: p. 272-288.
1038 18. Ulitsky, I. and D.P. Bartel, *lincRNAs: genomics, evolution, and mechanisms.* Cell, 2013.
1039 **154**(1): p. 26-46.
1040 19. Issler, O., et al., *Sex-Specific Role for the Long Non-coding RNA LINC00473 in*
1041 *Depression.* Neuron, 2020. **106**(6): p. 912-926 e5.
1042 20. Chen, Z., et al., *cAMP/CREB-regulated LINC00473 marks LKB1-inactivated lung cancer*
1043 *and mediates tumor growth.* J Clin Invest, 2016. **126**(6): p. 2267-79.
1044 21. Jiang, L.Y., et al., *CREB-induced LINC00473 promotes chemoresistance to TMZ in*
1045 *glioblastoma by regulating O6-methylguanine-DNA-methyltransferase expression via*
1046 *CEBPalpha binding.* Neuropharmacology, 2024. **243**: p. 109790.
1047 22. Ataman, B., et al., *Evolution of Osteocrin as an activity-regulated factor in the primate*
1048 *brain.* Nature, 2016. **539**(7628): p. 242-247.

1049 23. Pruunsild, P., et al., *Expression of the primate-specific LINC00473 RNA in mouse neurons*
1050 *promotes excitability and CREB-regulated transcription.* J Biol Chem, 2023. **299**(5): p.
1051 104671.
1052 24. Pruunsild, P., C.P. Bengtson, and H. Bading, *Networks of Cultured iPSC-Derived Neurons*
1053 *Reveal the Human Synaptic Activity-Regulated Adaptive Gene Program.* Cell Rep, 2017.
1054 **18**(1): p. 122-135.
1055 25. Tran, K.V., et al., *Human thermogenic adipocyte regulation by the long noncoding RNA*
1056 *LINC00473.* Nat Metab, 2020. **2**(5): p. 397-412.
1057 26. Glimcher, P.W. and A. Rustichini, *Neuroeconomics: the consilience of brain and decision.*
1058 Science, 2004. **306**(5695): p. 447-52.
1059 27. Kenning, P. and H. Plassmann, *Neuroeconomics: an overview from an economic*
1060 *perspective.* Brain Res Bull, 2005. **67**(5): p. 343-54.
1061 28. Loewenstein, G., S. Rick, and J.D. Cohen, *Neuroeconomics.* Annu Rev Psychol, 2008.
1062 **59**: p. 647-72.
1063 29. Kalenscher, T. and C.M. Pennartz, *Is a bird in the hand worth two in the future? The*
1064 *neuroeconomics of intertemporal decision-making.* Prog Neurobiol, 2008. **84**(3): p. 284-
1065 315.
1066 30. Clithero, J.A. and A. Rangel, *Informatic parcellation of the network involved in the*
1067 *computation of subjective value.* Soc Cogn Affect Neurosci, 2014. **9**(9): p. 1289-302.
1068 31. Levy, D.J. and P.W. Glimcher, *The root of all value: a neural common currency for choice.*
1069 Curr Opin Neurobiol, 2012. **22**(6): p. 1027-38.
1070 32. Louie, K. and P.W. Glimcher, *Efficient coding and the neural representation of value.* Ann
1071 N Y Acad Sci, 2012. **1251**: p. 13-32.
1072 33. Durand-de Cuttoli, R., et al., *A double-hit of social and economic stress in mice precipitates*
1073 *changes in decision-making strategies.* Biol Psychiatry, 2023.

34. Resulaj, A., et al., *Changes of mind in decision-making.* Nature, 2009. **461**(7261): p. 263-6.

35. Hare, T.A., C.F. Camerer, and A. Rangel, *Self-control in decision-making involves modulation of the vmPFC valuation system.* Science, 2009. **324**(5927): p. 646-8.

36. Alagapan, S., et al., *Cingulate dynamics track depression recovery with deep brain stimulation.* Nature, 2023. **622**(7981): p. 130-138.

37. Knutson, B., et al., *Neural responses to monetary incentives in major depression.* Biol Psychiatry, 2008. **63**(7): p. 686-92.

38. Holton, E., et al., *Goal commitment is supported by vmPFC through selective attention.* Nature Human Behaviour, 2024.

39. Sweis, B.M. and E.J. Nestler, *Pushing the boundaries of behavioral analysis could aid psychiatric drug discovery.* PLoS Biol, 2022. **20**(12): p. e3001904.

40. Sweis, B.M., M.J. Thomas, and A.D. Redish, *Beyond simple tests of value: measuring addiction as a heterogeneous disease of computation-specific valuation processes.* Learn Mem, 2018. **25**(9): p. 501-512.

41. Abram, S.V., et al., *The Web-Surf Task: A translational model of human decision-making.* Cogn Affect Behav Neurosci, 2016. **16**(1): p. 37-50.

42. Maisson, D., et al., *Widespread coding of navigational variables in prefrontal cortex* biorxiv, 2022.

43. McInnes, A.N., et al., *Psychometric validation and clinical correlates of an experiential foraging task.* BioRxiv, 2023. **2023.12.28.573439**.

44. Kazinka, R., A.W. MacDonald, 3rd, and A.D. Redish, *Sensitivity to Sunk Costs Depends on Attention to the Delay.* Front Psychol, 2021. **12**: p. 604843.

45. Abram, S.V., et al., *Neural signatures underlying deliberation in human foraging decisions.* Cogn Affect Behav Neurosci, 2019. **19**(6): p. 1492-1508.

46. Sweis, B.M., et al., *Sensitivity to "sunk costs" in mice, rats, and humans.* Science, 2018. **361**(6398): p. 178-181.

47. Steiner, A.P. and A.D. Redish, *Behavioral and neurophysiological correlates of regret in rat decision-making on a neuroeconomic task.* Nat Neurosci, 2014. **17**(7): p. 995-1002.

48. Durand-de Cuttoli, R., et al., *Distinct forms of regret linked to resilience versus susceptibility to stress are regulated by region-specific CREB function in mice.* Science Advances, 2022. **8**(42): p. eadd5579.

49. Redish, A.D., et al., *Sunk cost sensitivity during change-of-mind decisions is informed by both the spent and remaining costs.* Commun Biol, 2022. **5**(1): p. 1337.

50. Sweis, B.M., et al., *Altering gain of the infralimbic-to-accumbens shell circuit alters economically dissociable decision-making algorithms.* Proc Natl Acad Sci U S A, 2018. **115**(27): p. E6347-E6355.

51. Sweis, B.M., A.D. Redish, and M.J. Thomas, *Prolonged abstinence from cocaine or morphine disrupts separable valuations during decision conflict.* Nat Commun, 2018. **9**(1): p. 2521.

52. Diehl, G. and A.D. Redish, *Differential processing of decision information in subregions of rodent medial prefrontal cortex.* biorxiv, 2022.

53. Duin, A.A., et al., *Certainty and uncertainty of the future changes planning and sunk costs.* Behav Neurosci, 2021.

54. Schmidt, B., A.A. Duin, and A.D. Redish, *Disrupting the medial prefrontal cortex alters hippocampal sequences during deliberative decision making.* J Neurophysiol, 2019. **121**(6): p. 1981-2000.

55. Schmidt, B. and A.D. Redish, *Disrupting the medial prefrontal cortex with designer receptors exclusively activated by designer drug alters hippocampal sharp-wave ripples and their associated cognitive processes.* Hippocampus, 2021.

1124 56. Abram, S.V., A.D. Redish, and A.W. MacDonald, 3rd, *Learning From Loss After Risk:*
1125 *Dissociating Reward Pursuit and Reward Valuation in a Naturalistic Foraging Task.* Front
1126 Psychiatry, 2019. **10**: p. 359.
1127 57. Vialou, V., et al., *DeltaFosB in brain reward circuits mediates resilience to stress and*
1128 *antidepressant responses.* Nat Neurosci, 2010. **13**(6): p. 745-52.
1129 58. German, P.W. and H.L. Fields, *Rat nucleus accumbens neurons persistently encode*
1130 *locations associated with morphine reward.* J Neurophysiol, 2007. **97**(3): p. 2094-106.
1131 59. Sjulson, L., et al., *Cocaine Place Conditioning Strengthens Location-Specific*
1132 *Hippocampal Coupling to the Nucleus Accumbens.* Neuron, 2018. **98**(5): p. 926-934 e5.
1133 60. Nwakama, C.A., et al., *Diabetes alters neuroeconomically dissociable forms of mental*
1134 *accounting.* bioRxiv, 2024.
1135 61. Camille, N., et al., *The involvement of the orbitofrontal cortex in the experience of regret.*
1136 Science, 2004. **304**(5674): p. 1167-70.
1137 62. Coricelli, G., et al., *Regret and its avoidance: a neuroimaging study of choice behavior.*
1138 Nat Neurosci, 2005. **8**(9): p. 1255-62.
1139 63. Coricelli, G., R.J. Dolan, and A. Sirigu, *Brain, emotion and decision making: the*
1140 *paradigmatic example of regret.* Trends Cogn Sci, 2007. **11**(6): p. 258-65.
1141 64. Bardo, M.T. and R.A. Bevins, *Conditioned place preference: what does it add to our*
1142 *preclinical understanding of drug reward?* Psychopharmacology, 2000. **153**(1): p. 31-43.
1143 65. Tzschentke, T.M., *Measuring reward with the conditioned place preference (CPP)*
1144 *paradigm: update of the last decade.* Addict Biol, 2007. **12**(3-4): p. 227-462.
1145 66. Johnson, A. and A.D. Redish, *Neural ensembles in CA3 transiently encode paths forward*
1146 *of the animal at a decision point.* J Neurosci, 2007. **27**(45): p. 12176-89.
1147 67. Kay, K., et al., *Constant Sub-second Cycling between Representations of Possible*
1148 *Futures in the Hippocampus.* Cell, 2020. **180**(3): p. 552-567 e25.

1149 68. Huynh, T., et al., *Vicarious Trial-and-Error Is Enhanced During Deliberation in Human*
1150 *Virtual Navigation in a Translational Foraging Task.* Front Behav Neurosci, 2021. **15**: p.
1151 586159.
1152 69. Diehl, G. and A.D. Redish, *Measuring excitation-inhibition balance through spectral*
1153 *components of local field potentials.* bioRxiv, 2024.
1154 70. Kocharian, A., *Dopaminergic control of neuroeconomic decision-making.* ProQuest,
1155 University of Minnesota, 2023.
1156 71. Lind, E.B., et al., *A quadruple dissociation of reward-related behaviour in mice across*
1157 *excitatory inputs to the nucleus accumbens shell.* Commun Biol, 2023. **6**(1): p. 119.
1158 72. Barrot, M., et al., *CREB activity in the nucleus accumbens shell controls gating of*
1159 *behavioral responses to emotional stimuli.* Proc Natl Acad Sci U S A, 2002. **99**(17): p.
1160 11435-40.
1161 73. Carlezon, W.A., Jr., R.S. Duman, and E.J. Nestler, *The many faces of CREB.* Trends
1162 Neurosci, 2005. **28**(8): p. 436-45.
1163 74. Kim, J., et al., *Memory recall and modifications by activating neurons with elevated CREB.*
1164 Nat Neurosci, 2014. **17**(1): p. 65-72.
1165 75. Lonze, B.E. and D.D. Ginty, *Function and regulation of CREB family transcription factors*
1166 *in the nervous system.* Neuron, 2002. **35**(4): p. 605-23.
1167 76. McClung, C.A. and E.J. Nestler, *Regulation of gene expression and cocaine reward by*
1168 *CREB and DeltaFosB.* Nat Neurosci, 2003. **6**(11): p. 1208-15.
1169 77. Sakai, N., et al., *Inducible and brain region-specific CREB transgenic mice.* Mol
1170 Pharmacol, 2002. **61**(6): p. 1453-64.
1171 78. Lorsch, Z.S., et al., *Stress resilience is promoted by a Zfp189-driven transcriptional*
1172 *network in prefrontal cortex.* Nat Neurosci, 2019. **22**(9): p. 1413-1423.
1173 79. Durand-de Cuttoli, R., et al., *Chronic social stress induces isolated deficits in reward*
1174 *anticipation on a neuroeconomic foraging task.* biorxiv, 2022.

1175 80. Barrot, M., et al., *Regulation of anxiety and initiation of sexual behavior by CREB in the*
1176 *nucleus accumbens.* Proc Natl Acad Sci U S A, 2005. **102**(23): p. 8357-62.
1177 81. Dong, Y., et al., *CREB modulates excitability of nucleus accumbens neurons.* Nat
1178 Neurosci, 2006. **9**(4): p. 475-7.
1179 82. Zhou, J., et al., *Effects of Estrogen Treatment on Expression of Brain-Derived*
1180 *Neurotrophic Factor and cAMP Response Element-Binding Protein Expression and*
1181 *Phosphorylation in Rat Amygdaloid and Hippocampal Structures.* Neuroendocrinology,
1182 2005. **81**(5): p. 294-310.
1183 83. Sharma, K., et al., *Chronic exposure to estrogen and tamoxifen regulates synaptophysin*
1184 *and phosphorylated cAMP response element-binding (CREB) protein expression in CA1*
1185 *of ovariectomized rat hippocampus.* Brain Res, 2007. **1132**(1): p. 10-9.
1186 84. Lorsch, Z.S., et al., *Estrogen receptor alpha drives pro-resilient transcription in mouse*
1187 *models of depression.* Nat Commun, 2018. **9**(1): p. 1116.
1188 85. Shansky, R.M., et al., *Estrogen mediates sex differences in stress-induced prefrontal*
1189 *cortex dysfunction.* Mol Psychiatry, 2004. **9**(5): p. 531-8.
1190 86. Issler, O., et al., *The long noncoding RNA FEDORA is a cell type– and sex-specific*
1191 *regulator of depression.* Science Advances, 2022. **8**(48).
1192

Figure 1

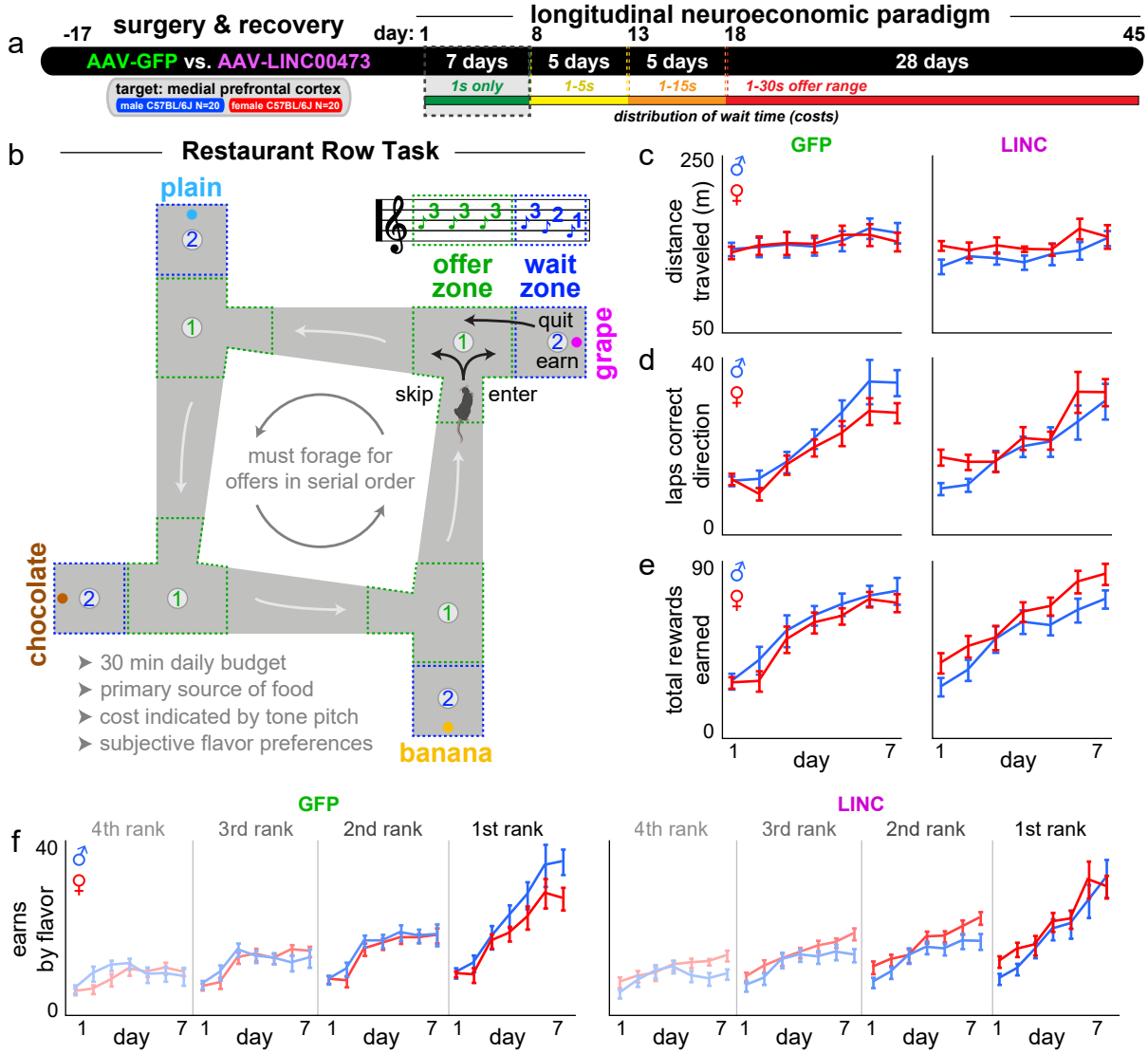
a
-17
surgery & recovery
AAV-GFP vs. AAV-LINC00473
target: medial prefrontal cortex
male C57BL/6J N=20
female C57BL/6J N=20
longitudinal neuroeconomic paradigm
day: 1
8
13
18
45
7 days
5 days
5 days
28 days
1s only
1-5s
1-15s
1-30s offer range
distribution of wait time (costs)
b
Restaurant Row Task
plain
offer zone
wait zone
quit
earn
grape
skip
enter
must forage for offers in serial order
chocolate
banana
30 min daily budget
primary source of food
cost indicated by tone pitch
subjective flavor preferences
c
GFP
LINC
distance traveled (m)
250
50
d
laps correct direction
40
0
e
total rewards earned
90
0
1
day
7
f
GFP
LINC
4th rank
3rd rank
2nd rank
1st rank
earns by flavor
40
0

Figure 2

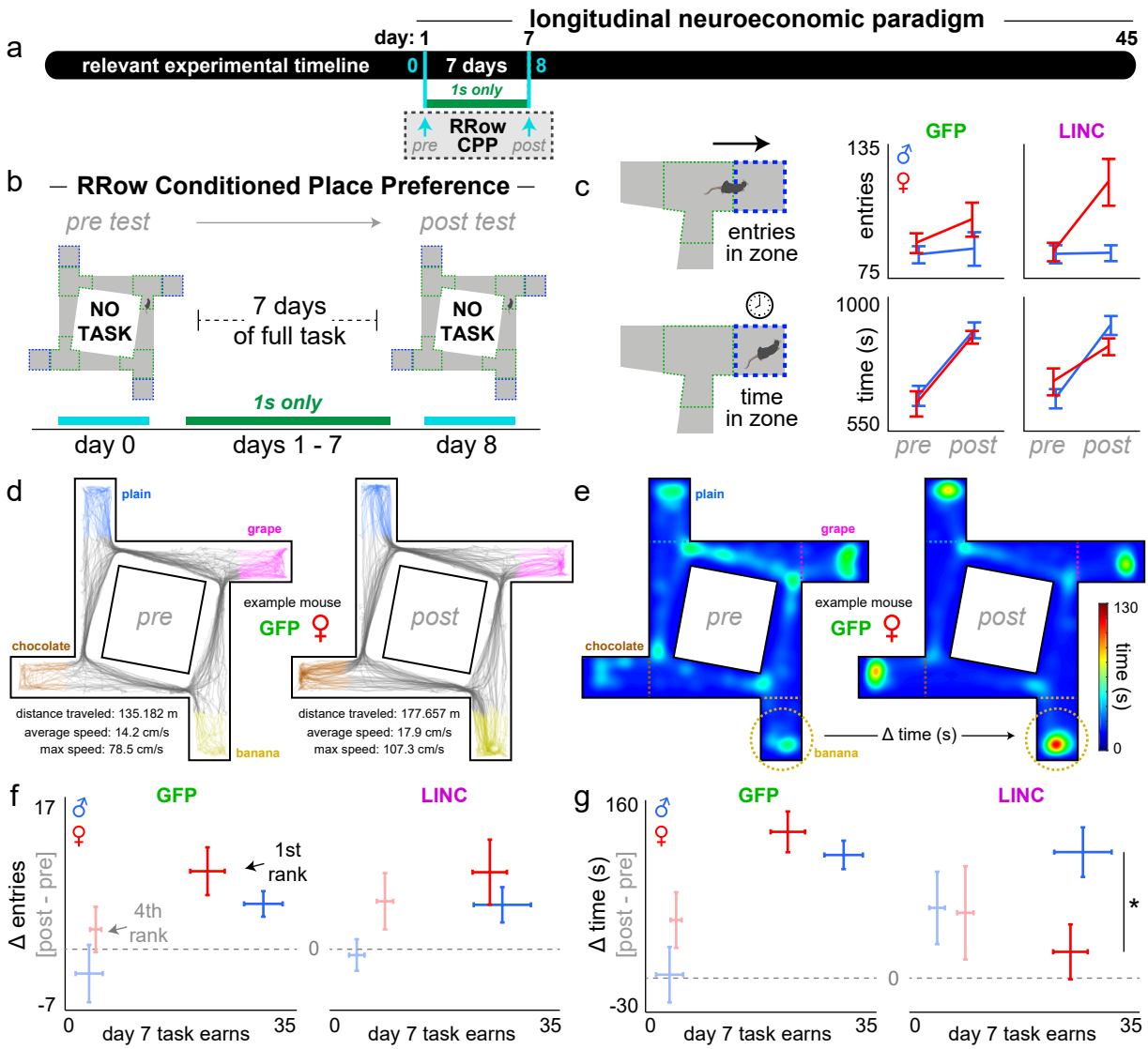
longitudinal neuroeconomic paradigm
a
day: 1
7
45
relevant experimental timeline
0
7 days
8
1s only
RRow CPP
pre
post
b
RRow Conditioned Place Preference
pre test
post test
NO TASK
7 days of full task
NO TASK
1s only
day 0
days 1 - 7
day 8
c
entries in zone
time in zone
GFP
LINC
entries
time (s)
135
75
1000
550
pre
post
d
plain
grape
chocolate
banana
pre
post
example mouse
GFP
distance traveled: 135.182 m
average speed: 14.2 cm/s
max speed: 78.5 cm/s
distance traveled: 177.657 m
average speed: 17.9 cm/s
max speed: 107.3 cm/s
e
Δ time (s)
130
0
time (s)
f
Δ entries [post - pre]
17
-7
1st rank
4th rank
day 7 task earns
0
35
g
Δ time (s) [post - pre]
160
-30
*

Figure 3

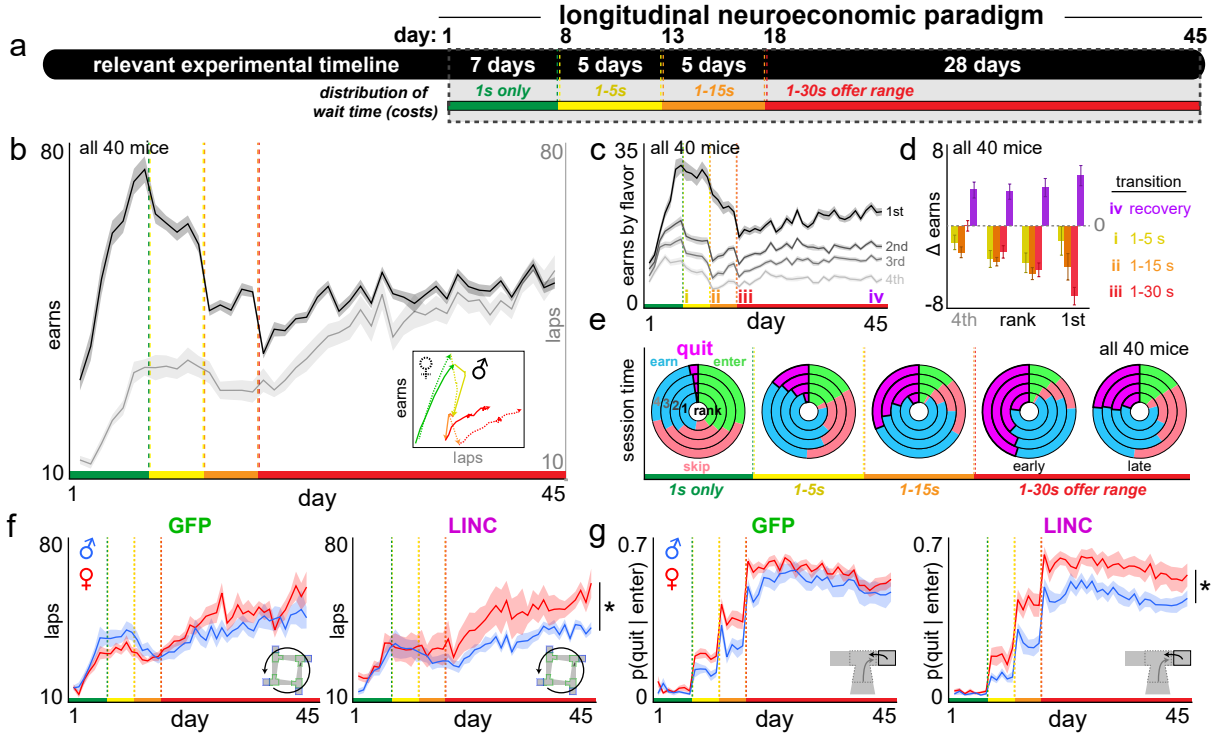
longitudinal neuroeconomic paradigm
a
day: 1
8
13
18
45
relevant experimental timeline
7 days
5 days
5 days
28 days
distribution of wait time (costs)
1s only
1-5s
1-15s
1-30s offer range
b
all 40 mice
earns
laps
day
c
all 40 mice
earns by flavor
1st
2nd
3rd
4th
i
ii
iii
iv
d
all 40 mice
Δ earns
transition
iv recovery
i 1-5 s
ii 1-15 s
iii 1-30 s
4th
rank
1st
e
quit
earn
enter
rank
skip
session time
all 40 mice
early
late
1s only
1-5s
1-15s
1-30s offer range
f
GFP
LINC
laps
day
g
GFP
LINC
p(quit | enter)
day

Figure 4

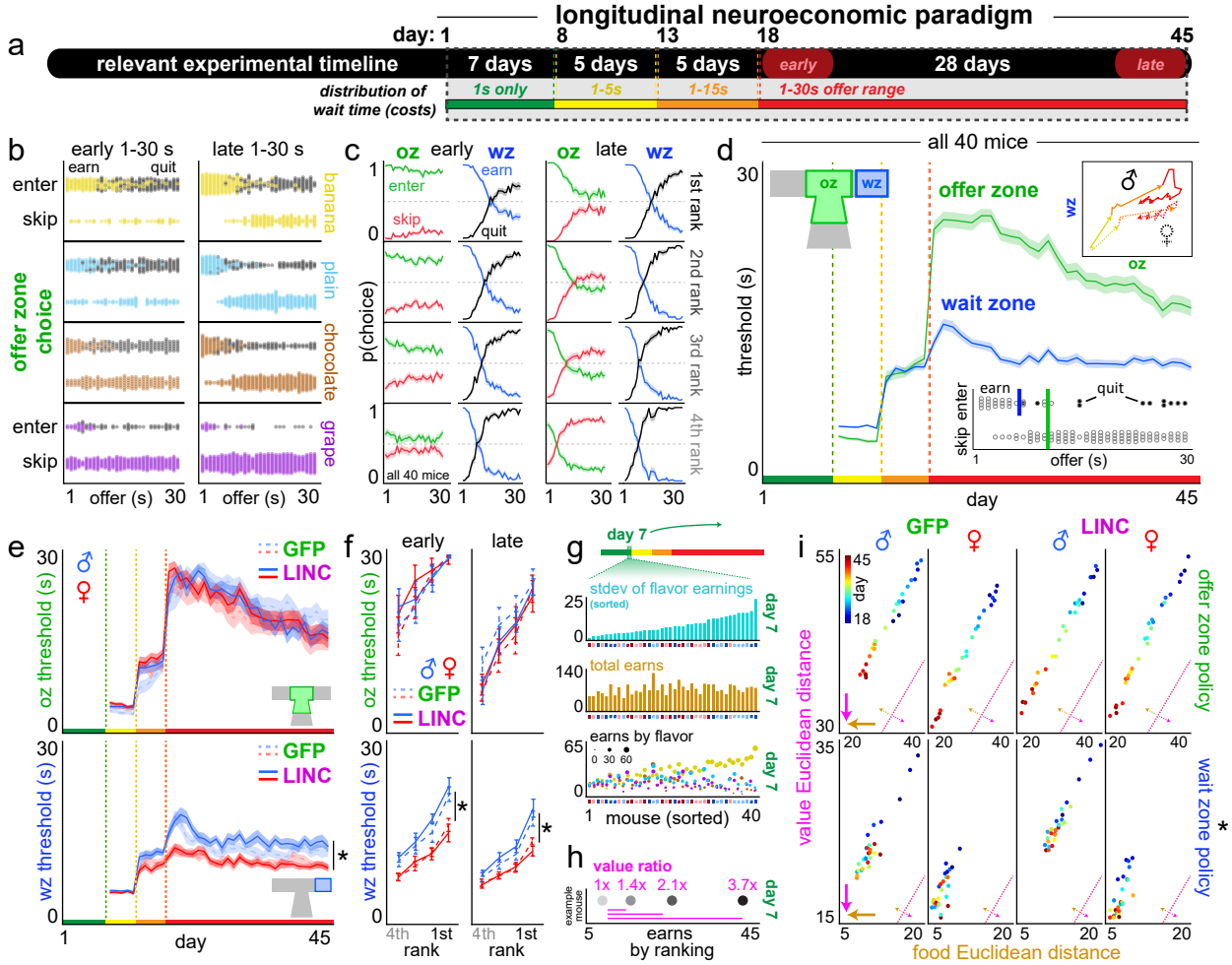
longitudinal neuroeconomic paradigm
a
day: 1
8
13
18
45
relevant experimental timeline
7 days
5 days
5 days
early
28 days
late
distribution of wait time (costs)
1s only
1-5s
1-15s
1-30s offer range
b
early 1-30 s
late 1-30 s
earn
quit
enter
skip
offer zone choice
banana
plain
chocolate
grape
offer (s)
c
oz
early
wz
late
enter
skip
earn
quit
p(choice)
1st rank
2nd rank
3rd rank
4th rank
all 40 mice
d
all 40 mice
offer zone
wz
oz
wait zone
threshold (s)
skip
enter
earn
quit
offer (s)
day
e
GFP
LINC
oz threshold (s)
wz threshold (s)
day
f
early
late
oz threshold (s)
wz threshold (s)
rank
g
day 7
stdev of flavor earnings
(sorted)
total earns
earns by flavor
mouse (sorted)
h
value ratio
1x 1.4x 2.1x
3.7x
example mouse
earns by ranking
i
GFP
LINC
day
value Euclidean distance
food Euclidean distance
offer zone policy
wait zone policy

Figure 5

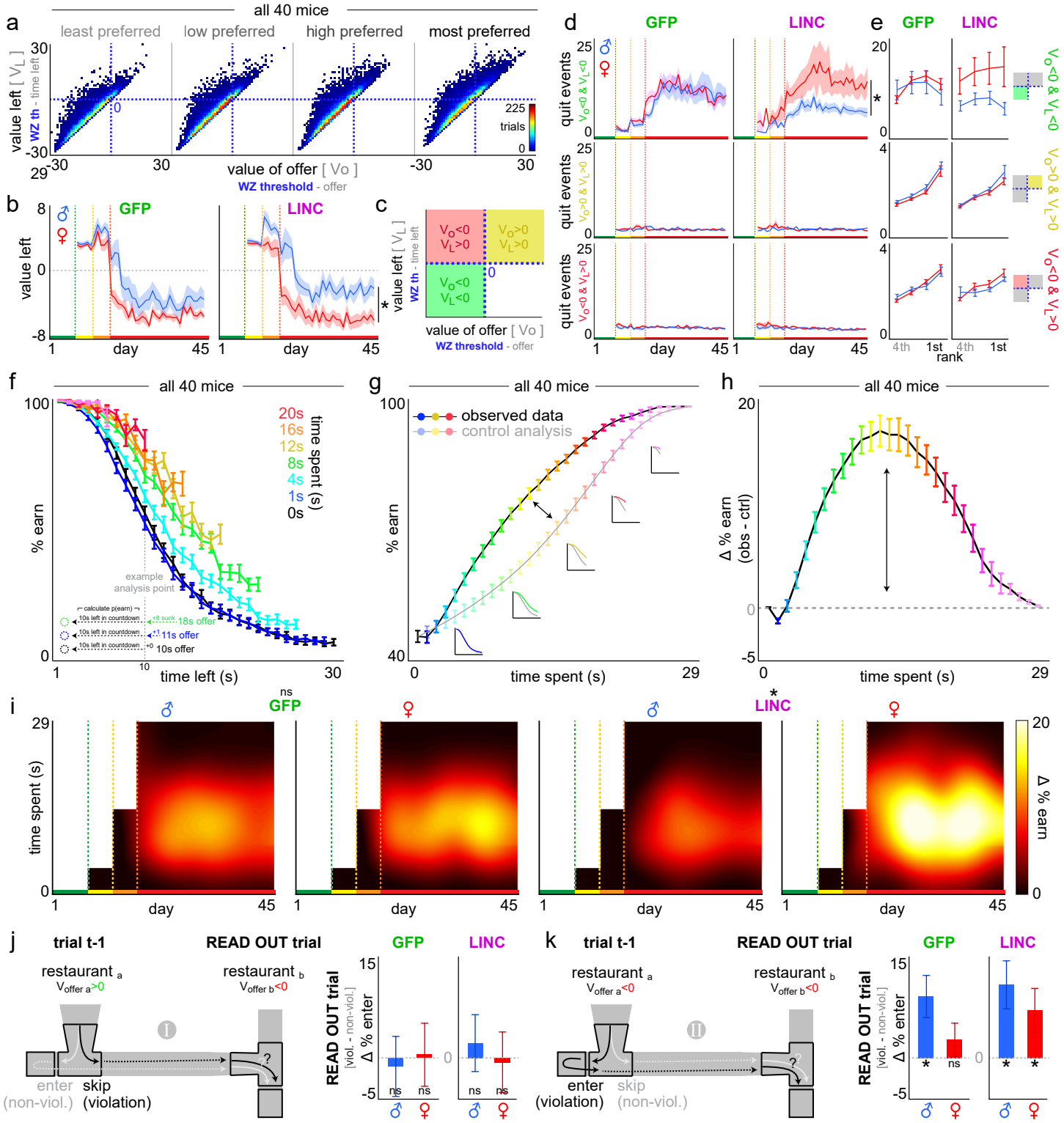
a
all 40 mice
least preferred
low preferred
high preferred
most preferred
value left [VL]
WZ th - time left
value of offer [Vo]
WZ threshold - offer
trials
b
GFP
LINC
value left
day
c
VO<0 VL>0
VO>0 VL>0
VO<0 VL<0
d
quit events
e
rank
f
all 40 mice
% earn
time spent (s)
20s
16s
12s
8s
4s
1s
0s
example analysis point
time left (s)
g
observed data
control analysis
h
Δ % earn (obs - ctrl)
i
ns
LINC
Δ % earn
j
trial t-1
READ OUT trial
restaurant a
restaurant b
enter (non-viol.)
skip (violation)
Δ % enter
[viol. - non-viol.]
k
enter (violation)
skip (non-viol.)

Figure 6

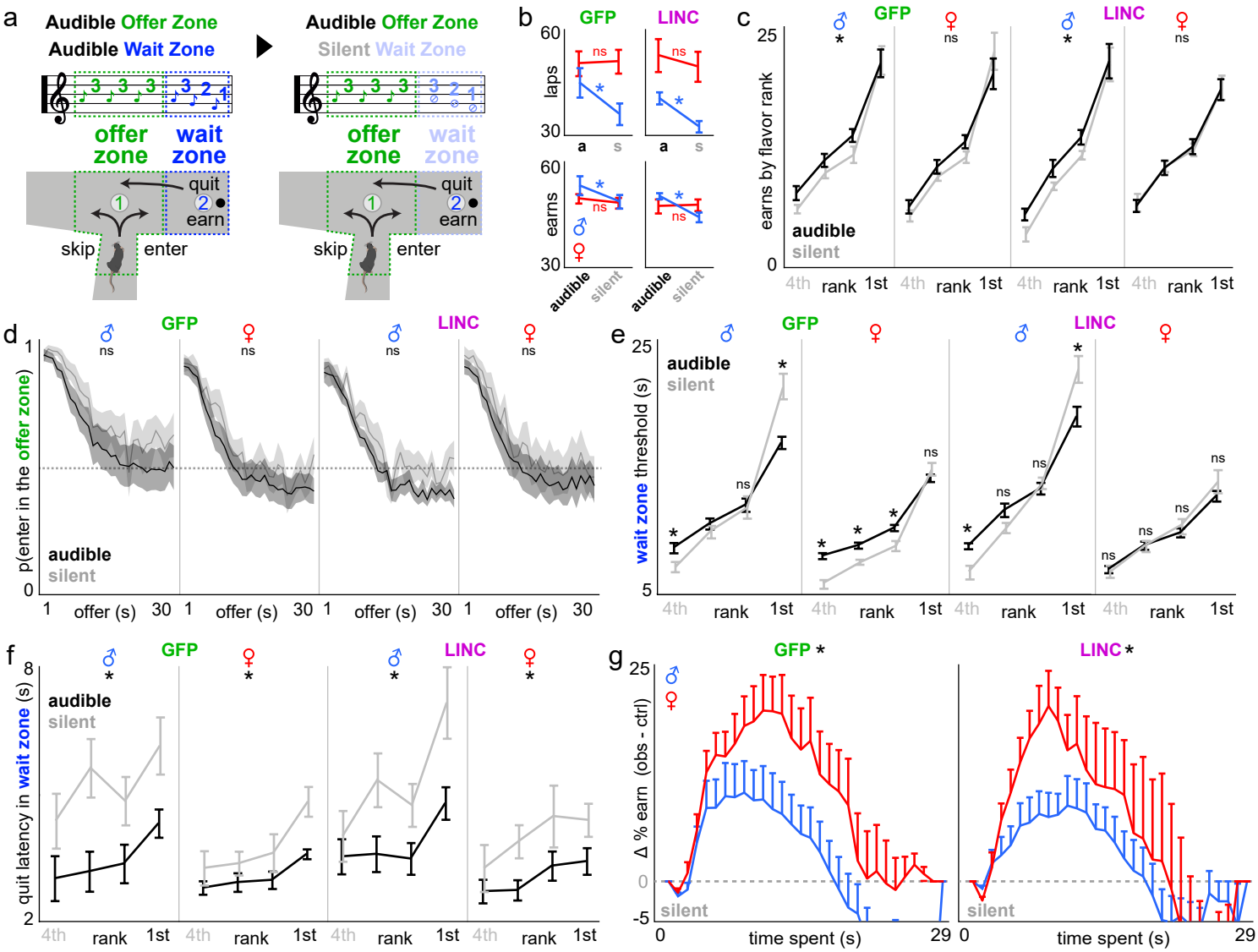
a
Audible Offer Zone
Audible Wait Zone
offer zone
wait zone
quit
earn
skip
enter
Audible Offer Zone
Silent Wait Zone
b
GFP
LINC
laps
earns
audible
silent
c
GFP
LINC
earns by flavor rank
audible
silent
4th rank 1st
d
GFP
LINC
p(enter in the offer zone)
audible
silent
offer (s)
e
GFP
LINC
wait zone threshold (s)
audible
silent
f
GFP
LINC
quit latency in wait zone (s)
audible
silent
g
GFP
LINC
Δ % earn (obs - ctrl)
silent
time spent (s)

Supplementary Figure 1

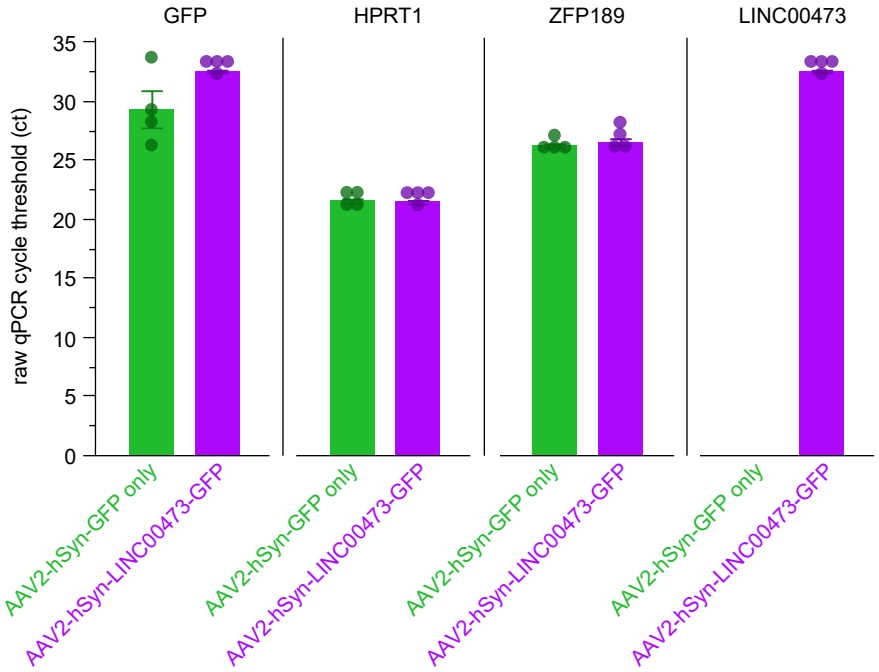

Supplementary Figure 2

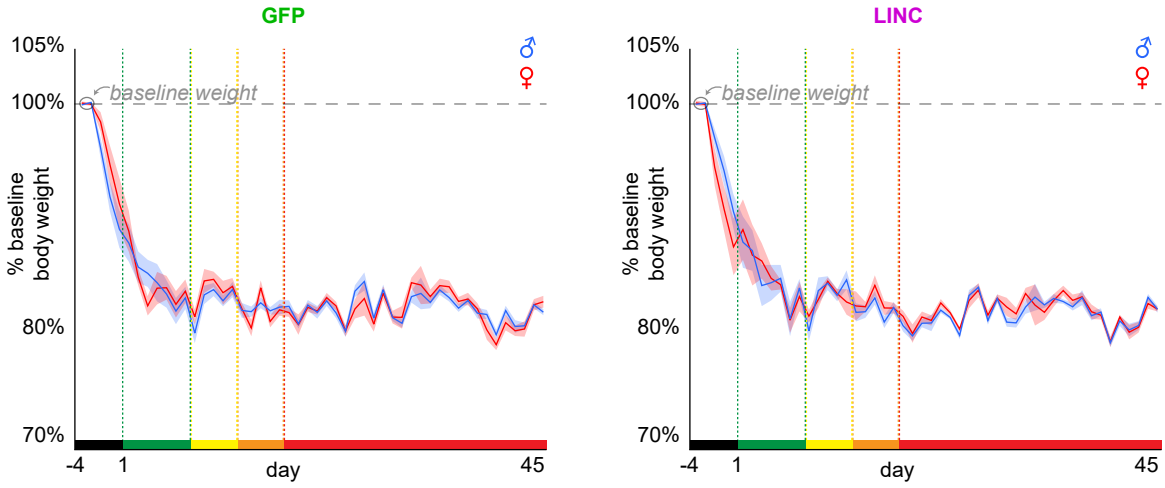

Supplementary Figure 3

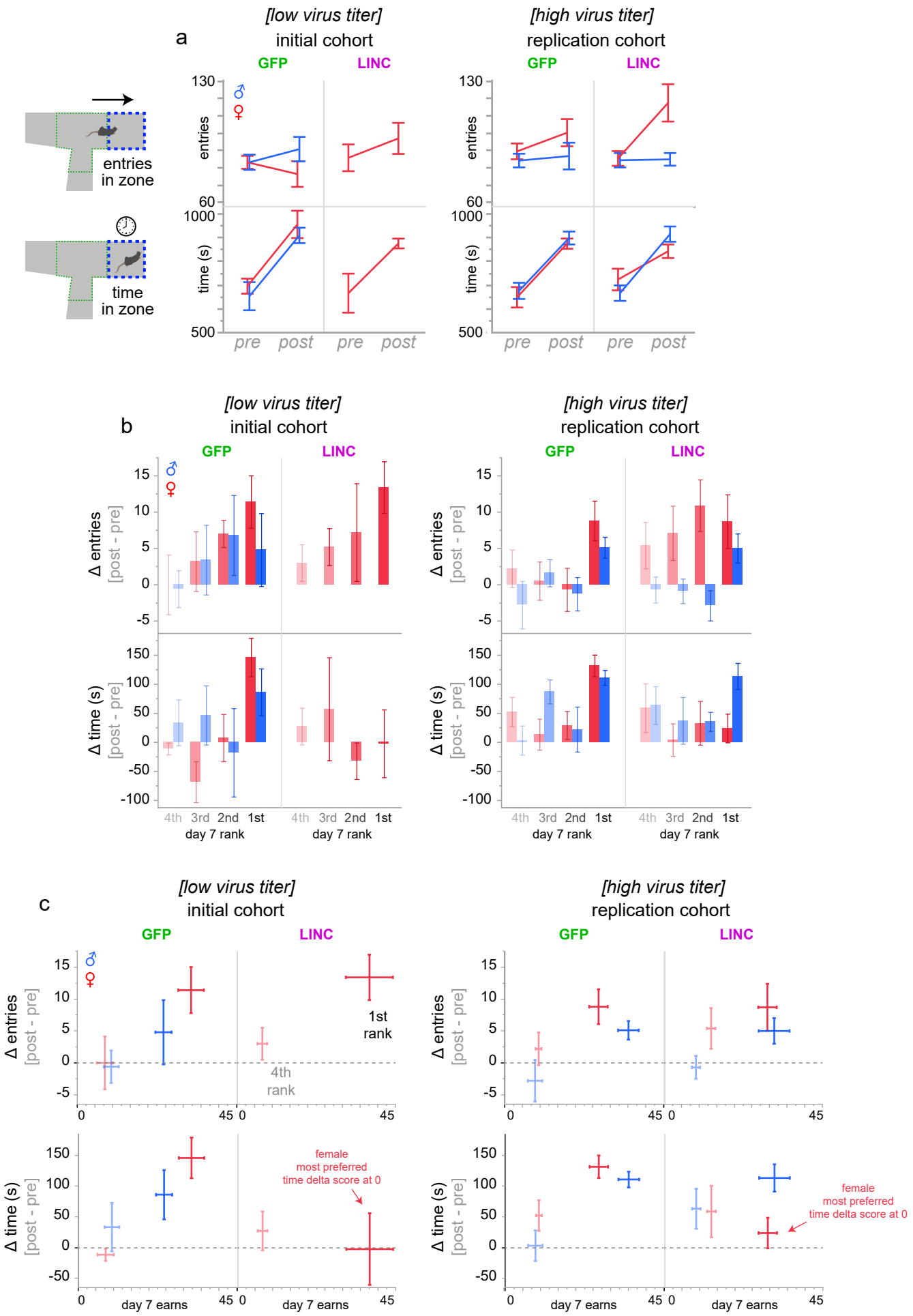

Supplementary Figure 4

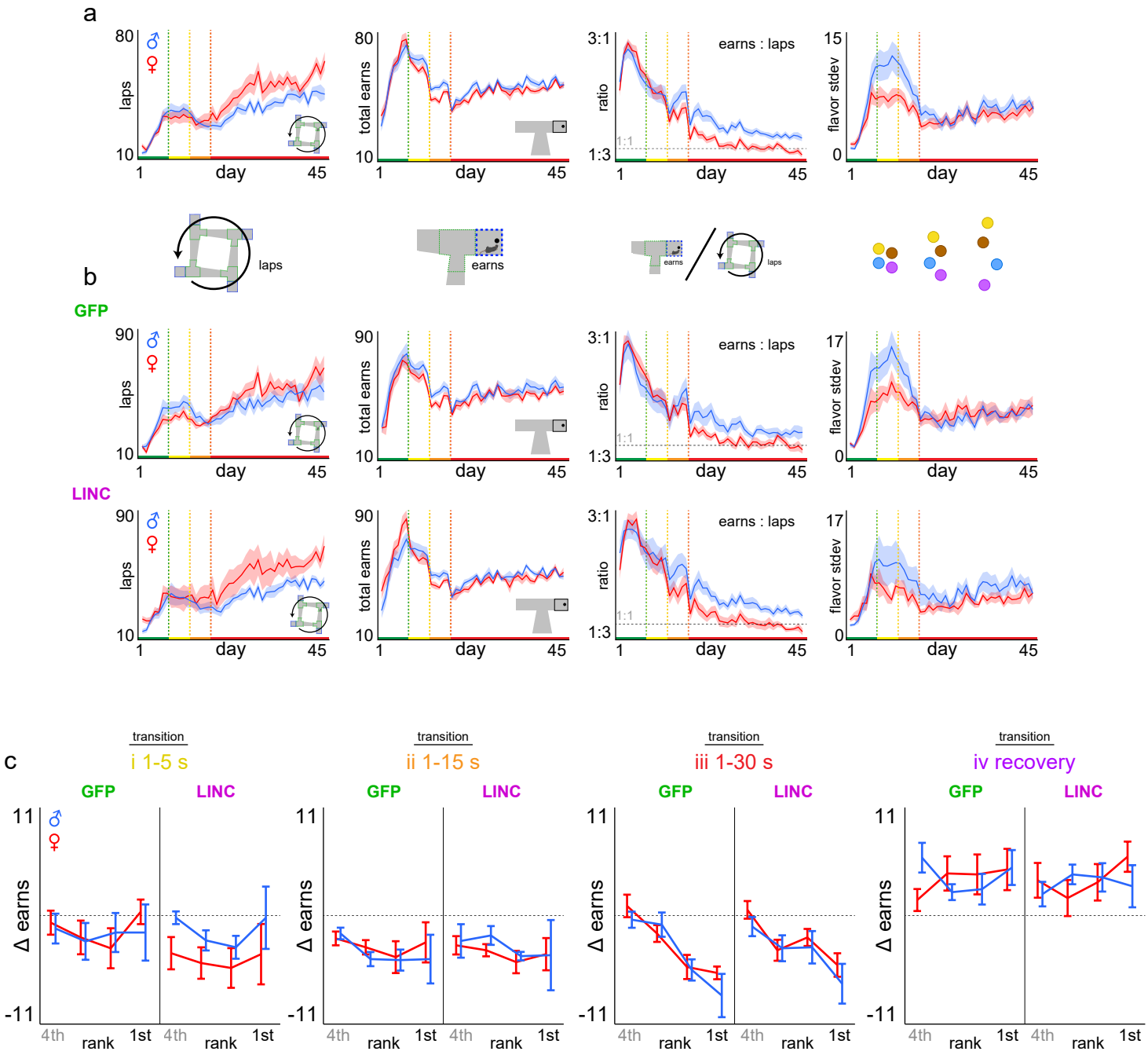

Supplementary Figure 5

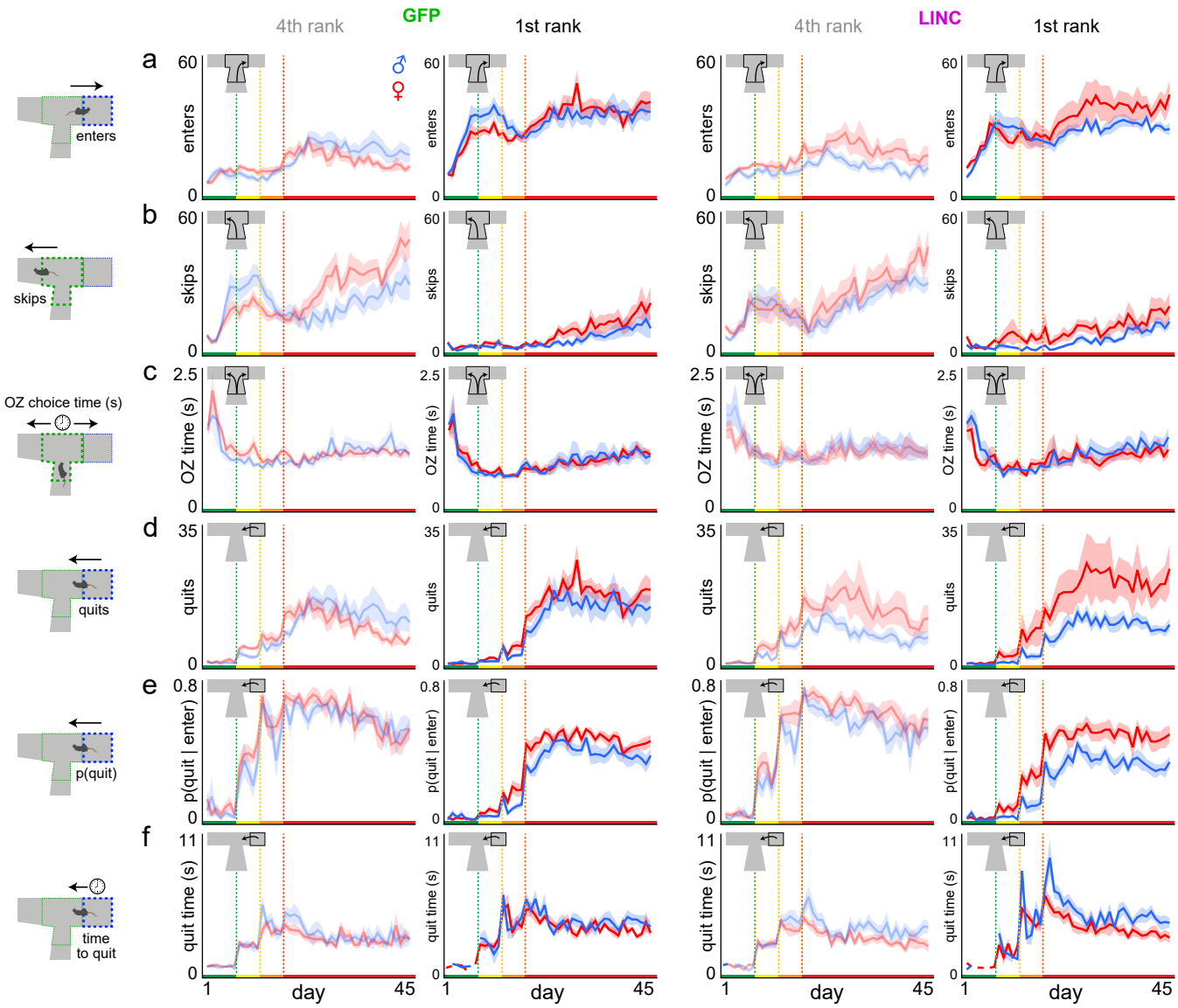

Supplementary Figure 6

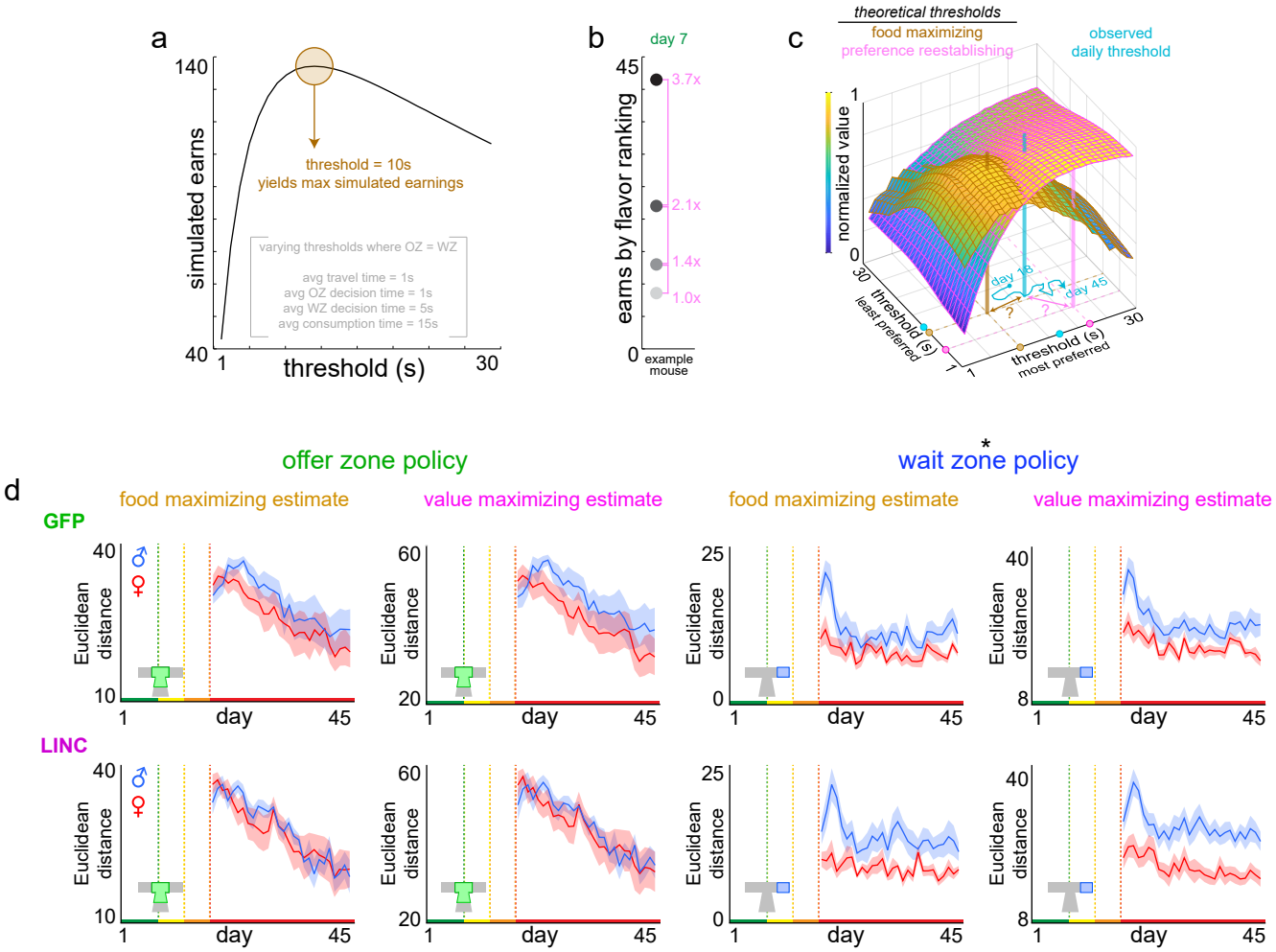

Supplementary Fig. 7

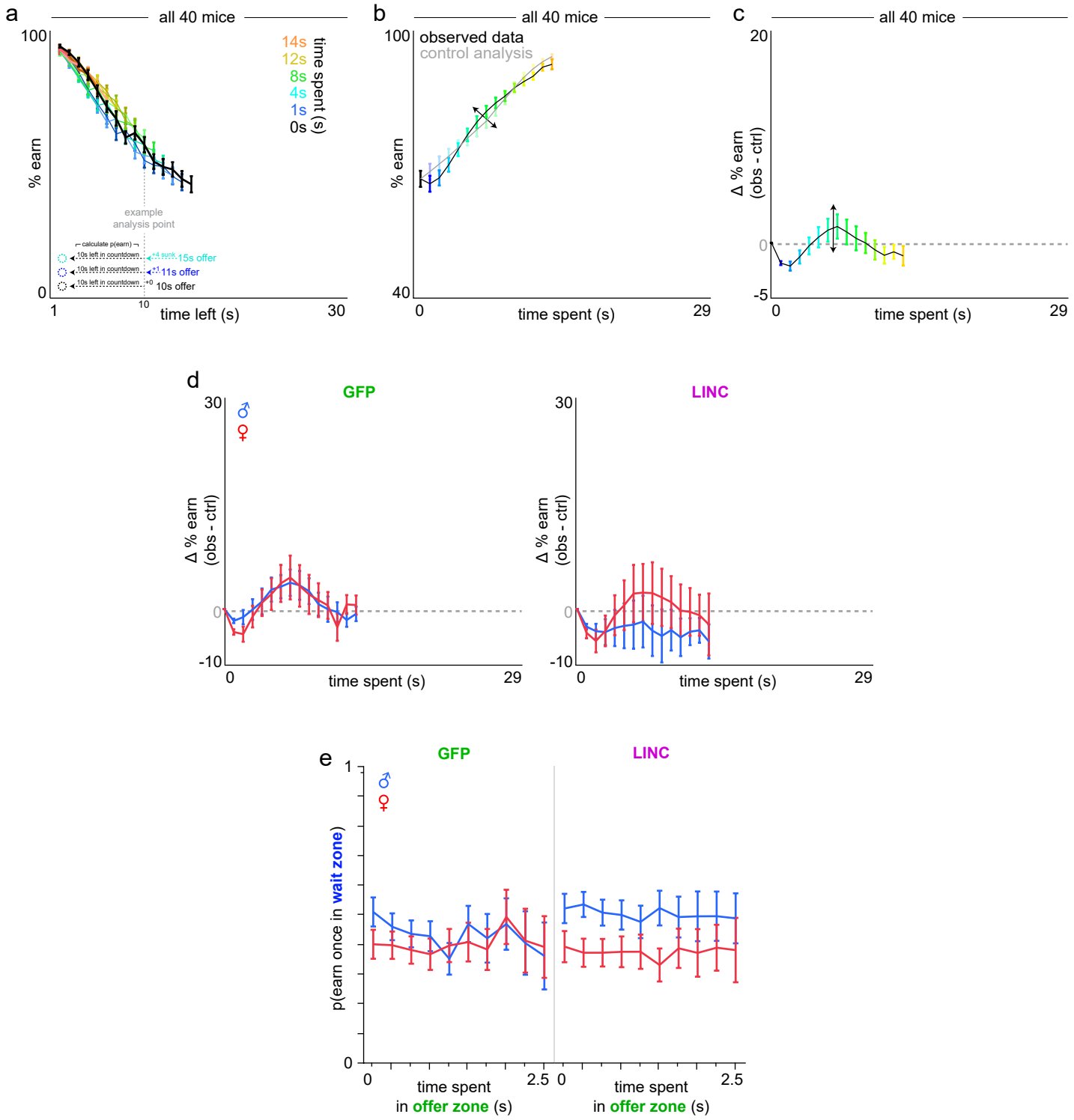
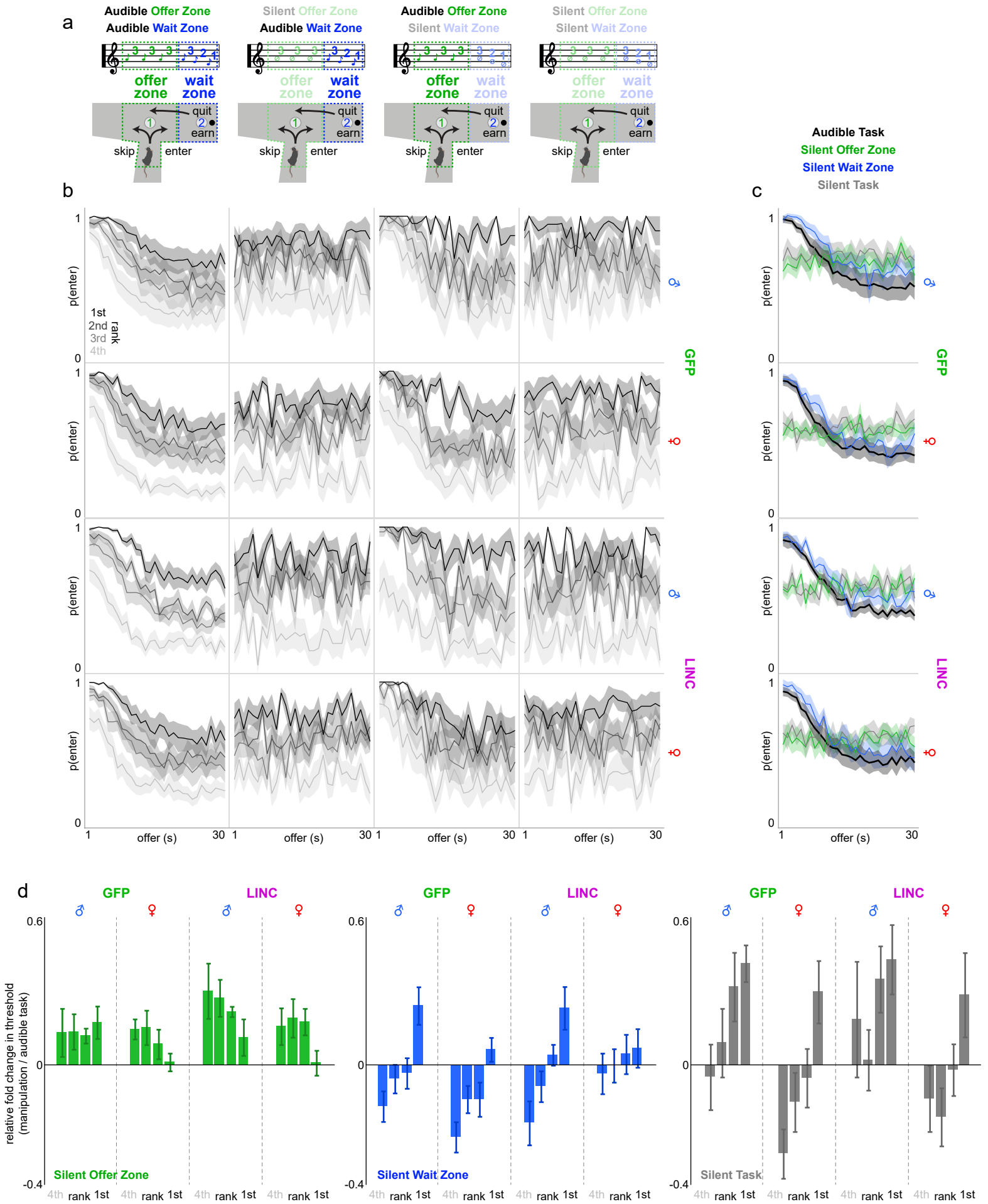
Supplementary Fig. 8